Exchange and polarization effects on elastic electron-atom/ion scattering

(aka. ***a small part of a bigger project****)*

Constantine E. Theodosiou
Department of Physics and Astronomy
University of Toledo (USA)

Students: Yuriy Sosov
Mehrdad Adibzadeh
Angel Acosta-Colon

*Supported by the US National Science Foundation

The objectives:

- understand the physics of weakly-ionized gases
- develop tools for optimizing the efficiency of Plasma Display Panels (PDPs)

Tools used:

- A combination of experimental and theoretical approaches

Needed for modeling and simulations :

- accurate atomic and molecular data (σ, $d\sigma/d\Omega$, τ, rates)
- accurate beam-surface interaction characteristics data (γ)
- accurate statistical description of the collisions in a non-thermal equilibrium environment ($f(v)$).

EPI prototype color AC PDP - 30 inch (diagonal)

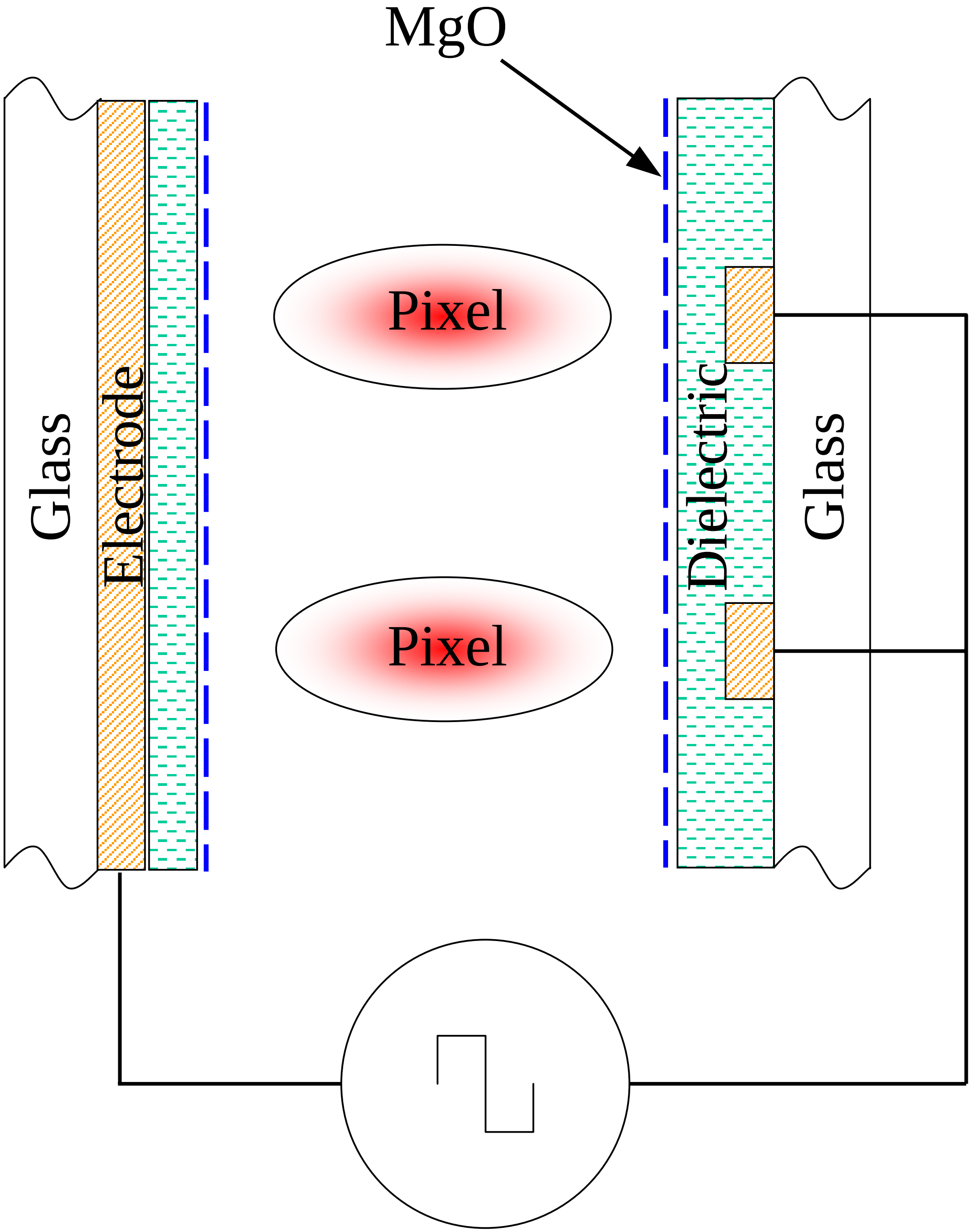

MgO
Pixel
Pixel
Glass
Electrode
Dielectric
Glass

Co-planar plasma display panel pixel

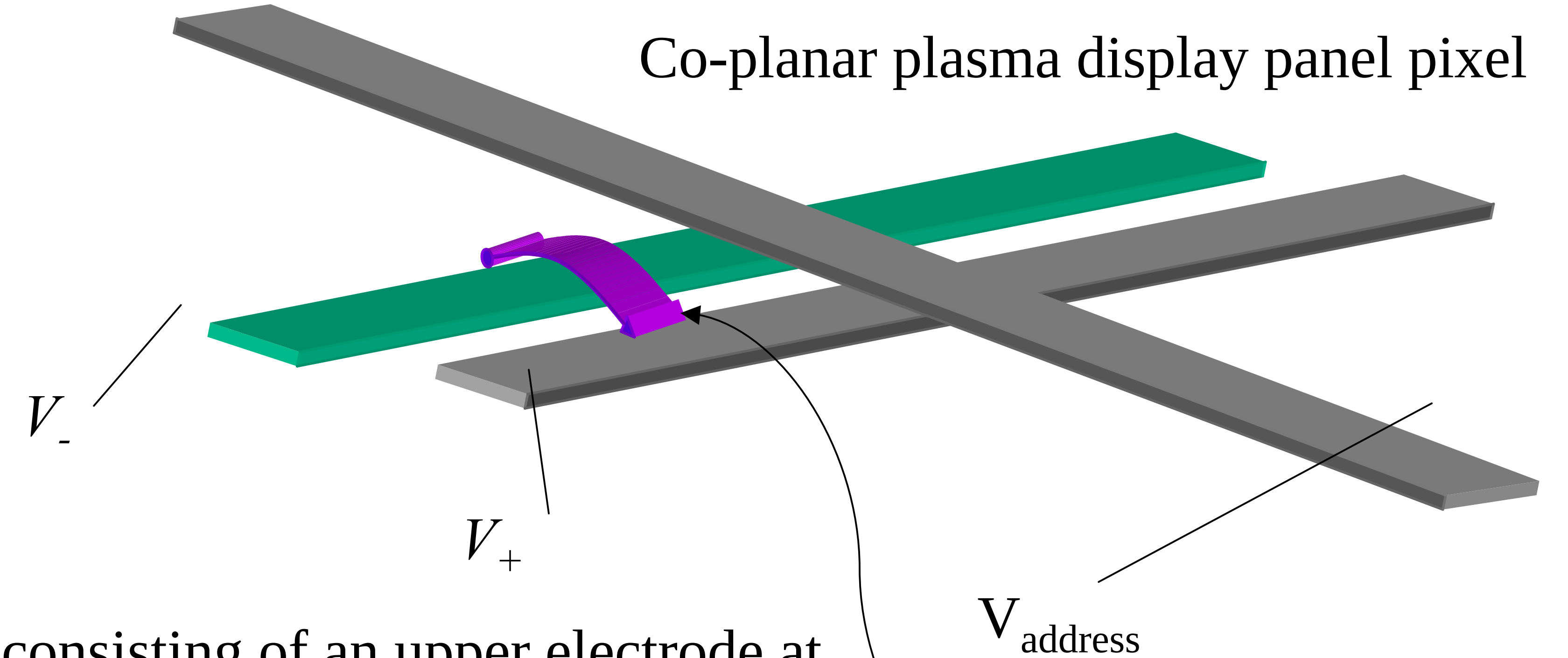

consisting of an upper electrode at constant potential, and two lower (parallel) electrodes with an alternating potential difference

Discharge occurs between parallel electrodes

Setup of our general problem

plasma physics is like astrophysics:

you need to know

- hydrodynamics
- statistical physics
- atomic physics
- molecular physics
- beam-surface interactions

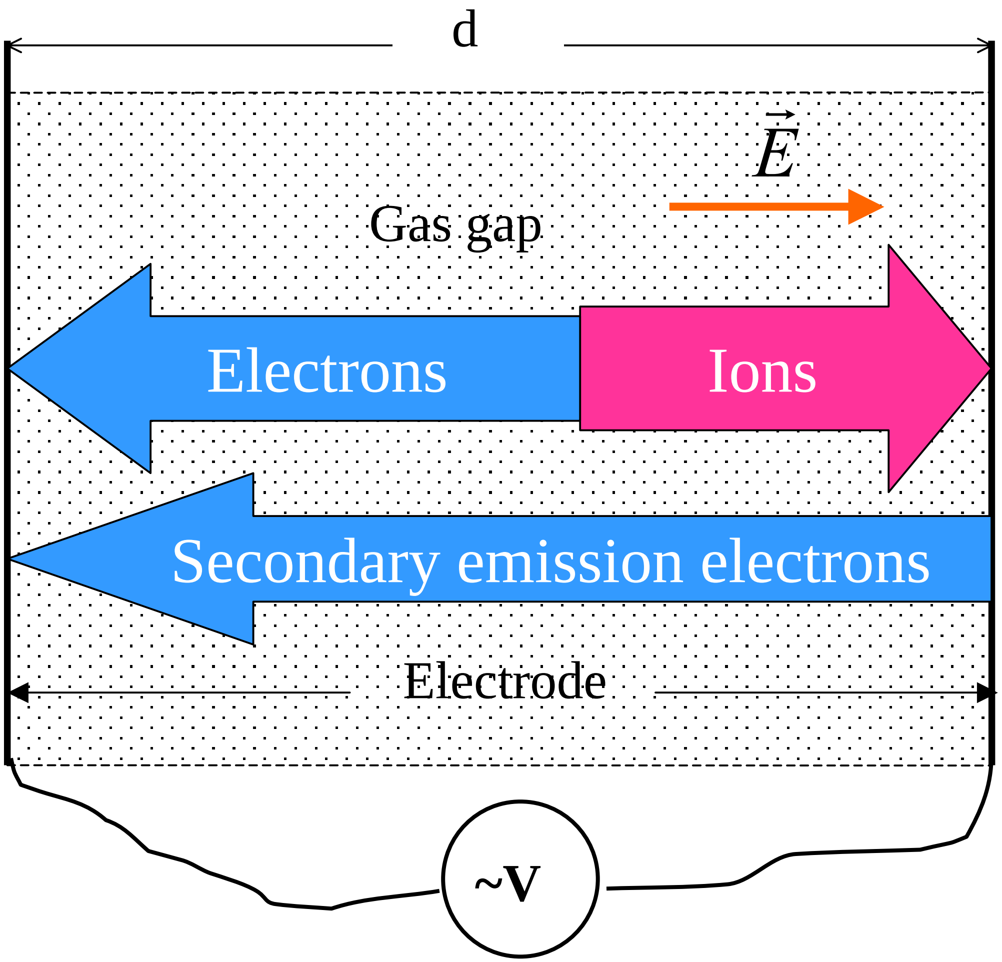

Boundary conditions

- Densities of all species = 0 at the boundaries
- For secondary electrons, $J_e = -\sum_i \gamma_i J_i$

Equations

$$\frac{\partial n_e}{\partial t} + \frac{\partial J_e}{\partial x} = S_e$$

$$\frac{\partial n_i}{\partial t} + \frac{\partial J_i}{\partial x} = S_i$$

$$\frac{\partial n_n}{\partial t} + \frac{\partial J_n}{\partial x} = S_n$$

$$J_e = n_e \mu_e E - \frac{\partial (D_e n_e)}{\partial x}$$

$$J_i = n_i \mu_i E - \frac{\partial (D_i n_i)}{\partial x}$$

$$J_n = -\frac{\partial (D_n n_n)}{\partial x}$$

$$\frac{dE}{dx} = \frac{e}{\varepsilon_0}(n_e - n_p)$$

11 equation for species coupled with 1 for electric field

Information needed and used as input to the solution

- **Electron collision rates**

found by solving the Boltzmann equation in stationary electric field for two-term expansion

$$S = \alpha(E/p)J_e$$

- **Chemical reaction rates**

$$A + B \rightarrow C$$

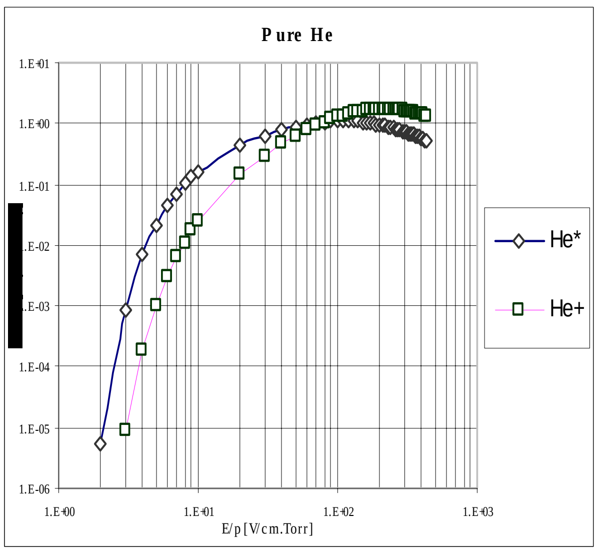

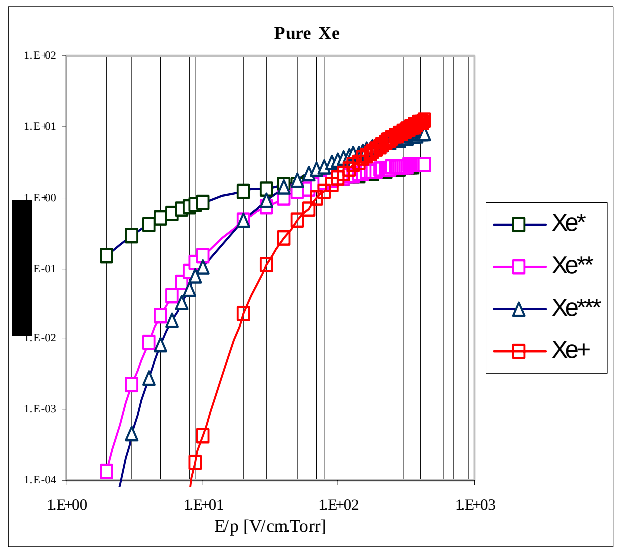

$$rate = k[A][B]$$

$$S_A = -rate,$$

$$S_B = -rate,$$

$$S_C = rate$$

- **Secondary electron coefficients** $\gamma_i \; , \gamma_n$.

Species and reactions for He Xe mixture

Electrons,

Ions: He^+, Xe^+, He_2^+, Xe_2^+

Neutrals: He^*, Xe^*, Xe^{**}, Xe^{***}, He_2, Xe_2

Process	Process	Process
Electron impact excitation	Electron impact ionisation	Charge exchange in
of atoms in the ground state	*of atoms in excited states*	two-body heavy particle collisions
e + He->He* + e	e + He*->He+ + 2e	*of atoms and molecules*
e + Xe->Xe* + e	e + Xe*->Xe+ + 2e	He2+ + Xe ->Xe+ +2He
e + Xe->Xe** + e	e + Xe**->Xe+ + 2e	
e + Xe->Xe*** + e	e + Xe***->Xe+ + 2e	Excited molecule formation in
		three-body heavy particle collisions
Electron impact de-excitation	Electron impact ionisation	*of atoms*
of ecited atoms to the ground state	*of excited molecules*	He* + 2He -> He2* + He
e + He*->He + e	e + He2*->He2+ + 2e	He* + He + Xe -> He2* + Xe
e + Xe*->Xe + e	e + Xe2*->Xe2+ + 2e	Xe* + 2Xe -> Xe2* + Xe
e + Xe**->Xe + e		Xe** + 2Xe -> Xe2* + Xe
e + Xe***->Xe + e	Electron impact recombination	Xe*** + 2Xe -> Xe2* + Xe
	of molecules	Xe* + He + Xe -> Xe2* + He
Electron impact excitation	e + He2+ -> He* + He	Xe** + He + Xe -> Xe2* + He
of atoms in excited states to a higher excited state	e + Xe2+ -> Xe* + Xe	Xe*** + He + Xe -> Xe2* + He
e + Xe*->Xe** + e	e + Xe2+ -> Xe** + Xe	
e + Xe*->Xe*** + e	e + Xe2+ -> Xe*** + Xe	Ionised molecule formation in
e + Xe**->Xe*** + e		three-body heavy particle collisions
	Ions formation in	*of atoms and ions*
Electron impact de-excitation	two-body heavy particle collisions	He+ + 2He -> He2+ + He
of atoms in excited states to a lower excited state	*of atoms*	Xe+ + 2Xe -> Xe2+ + Xe
e + Xe**->Xe* + e	2He* -> He+ + He +e	Xe+ + He + Xe -> Xe2+ + He
e + Xe***->Xe* + e	2Xe* -> Xe+ + Xe +e	
e + Xe***->Xe** + e	2Xe** -> Xe+ + Xe +e	UV Radiation
	2Xe*** -> Xe+ + Xe +e	Xe2*->2Xe+hv
Electron impact ionisation	He* + Xe -> Xe+ + He + e	Xer*->Xe+hv
of atoms in the ground state	*of atoms and molecules*	Xer**->Xe+hv
e + He->He+ + 2e	He2* + Xe -> Xe+ + 2He + e	
e + Xe->Xe+ + 2e		

Ne-Xe reaction scheme

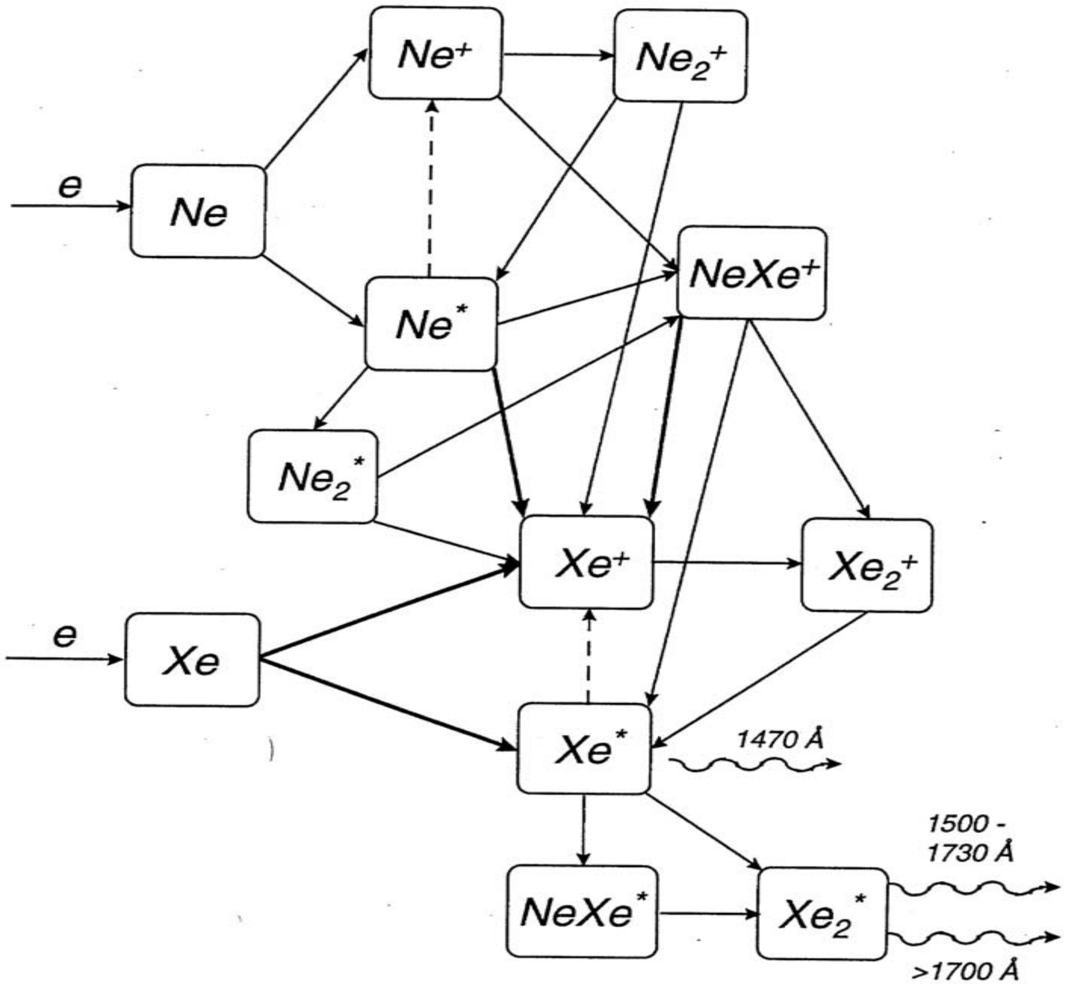

Xe - vuv emission process

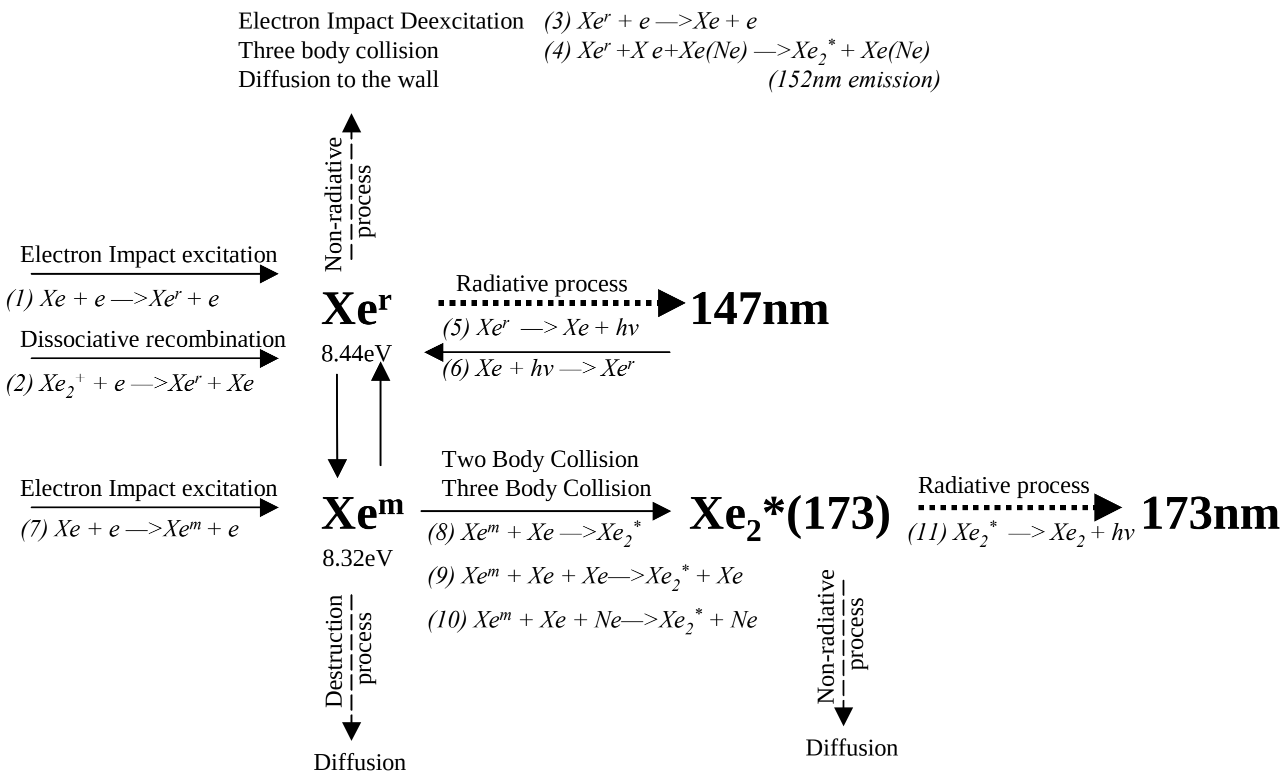

$$\frac{\partial f}{\partial t} + \frac{\partial}{\partial x_i}(f\, v_i) + \frac{\partial}{\partial v_i}(f\, \dot{v}_i) = (\frac{df}{dt})_{\text{collisional}}$$

Requires accurate knowledge of many processes in

- atomic physics
- molecular physics
- beam-surface interactions

Elastic cross sections

are among the most important

Work by the Greifswald Plasma Group has shown [e.g., Leyh et al. Comput. Phys. Rev. Commun. **113**, 33 (1998)] that:

- anisotropic vs. isotropic elastic (and inelastic) collisions can make a big difference in the electron velocity distribution of electrons in weakly ionized plasmas

simulations

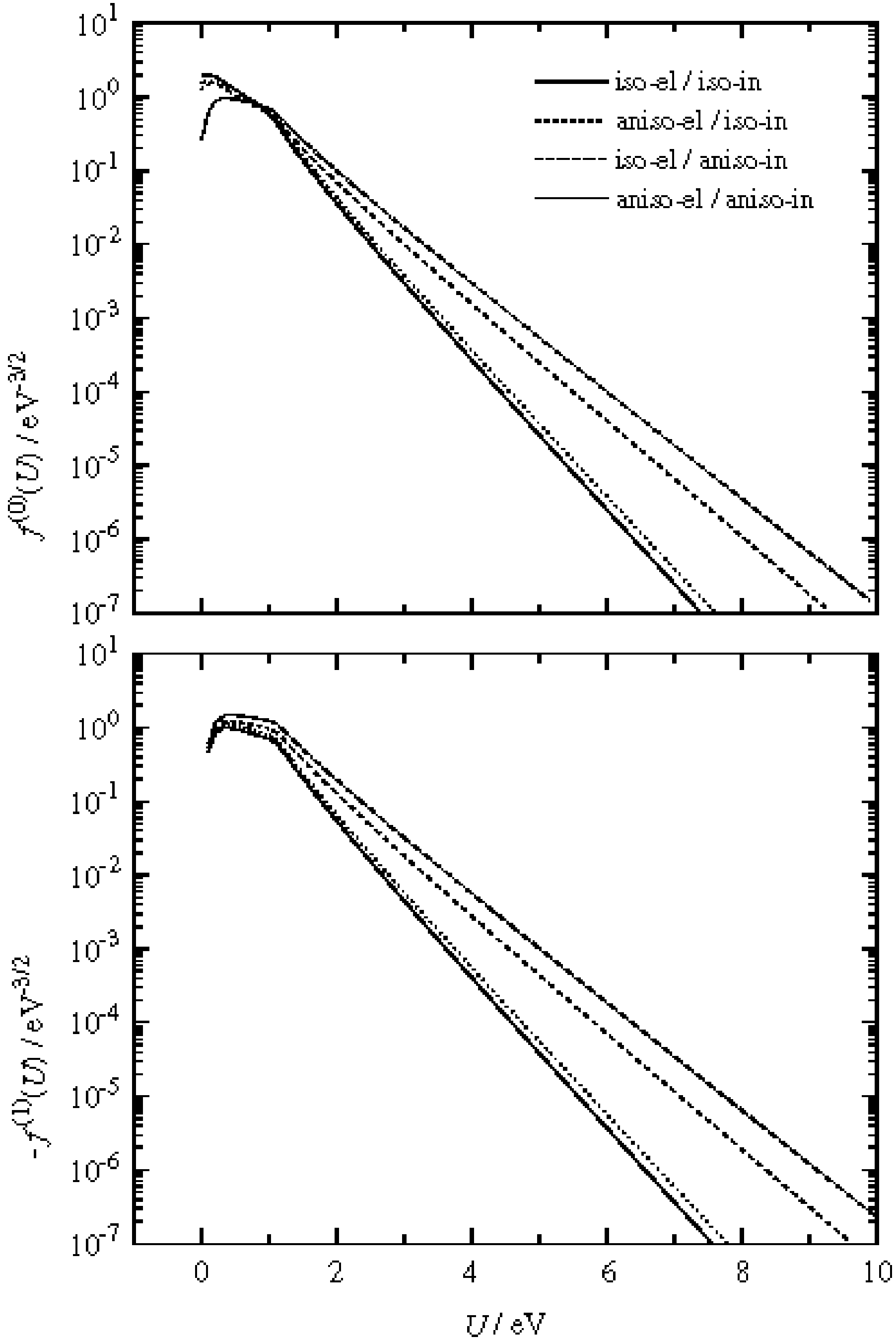

Greeenwood et al., [Phys. Rev. Lett. **75**, 1062 (1995)] claimed backward elastic scattering of 3.3 eV electrons on Ar^+ measurements in disagreement with theory

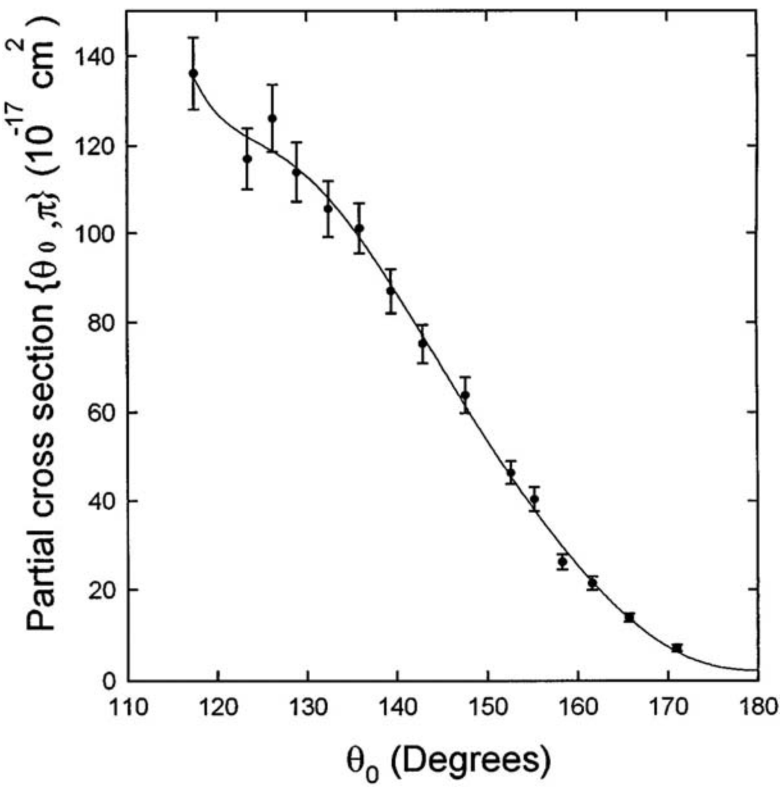

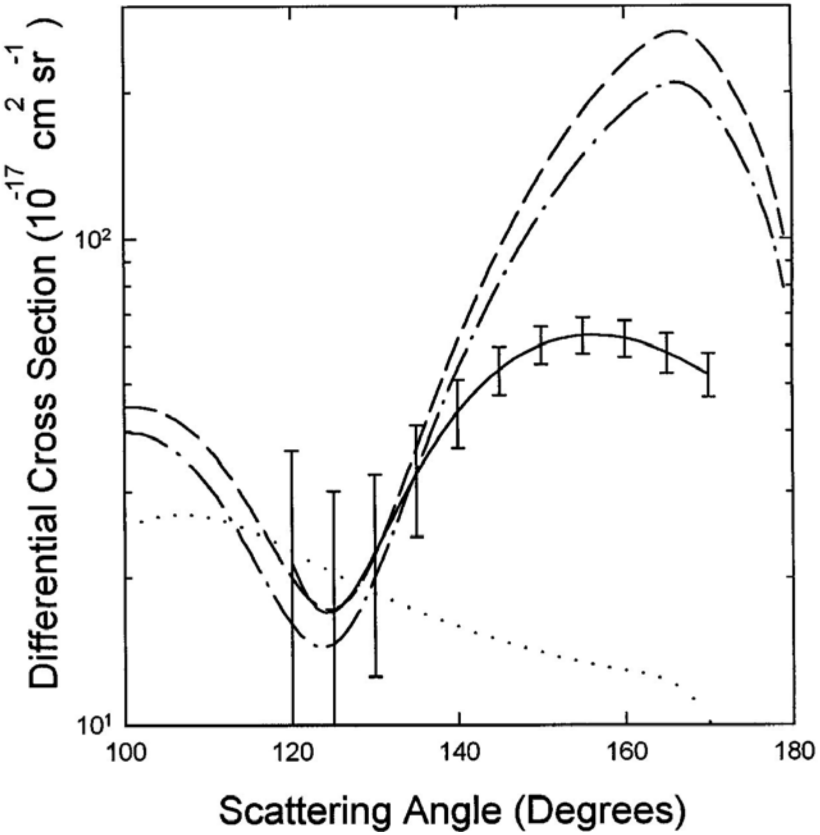

Problems – 2

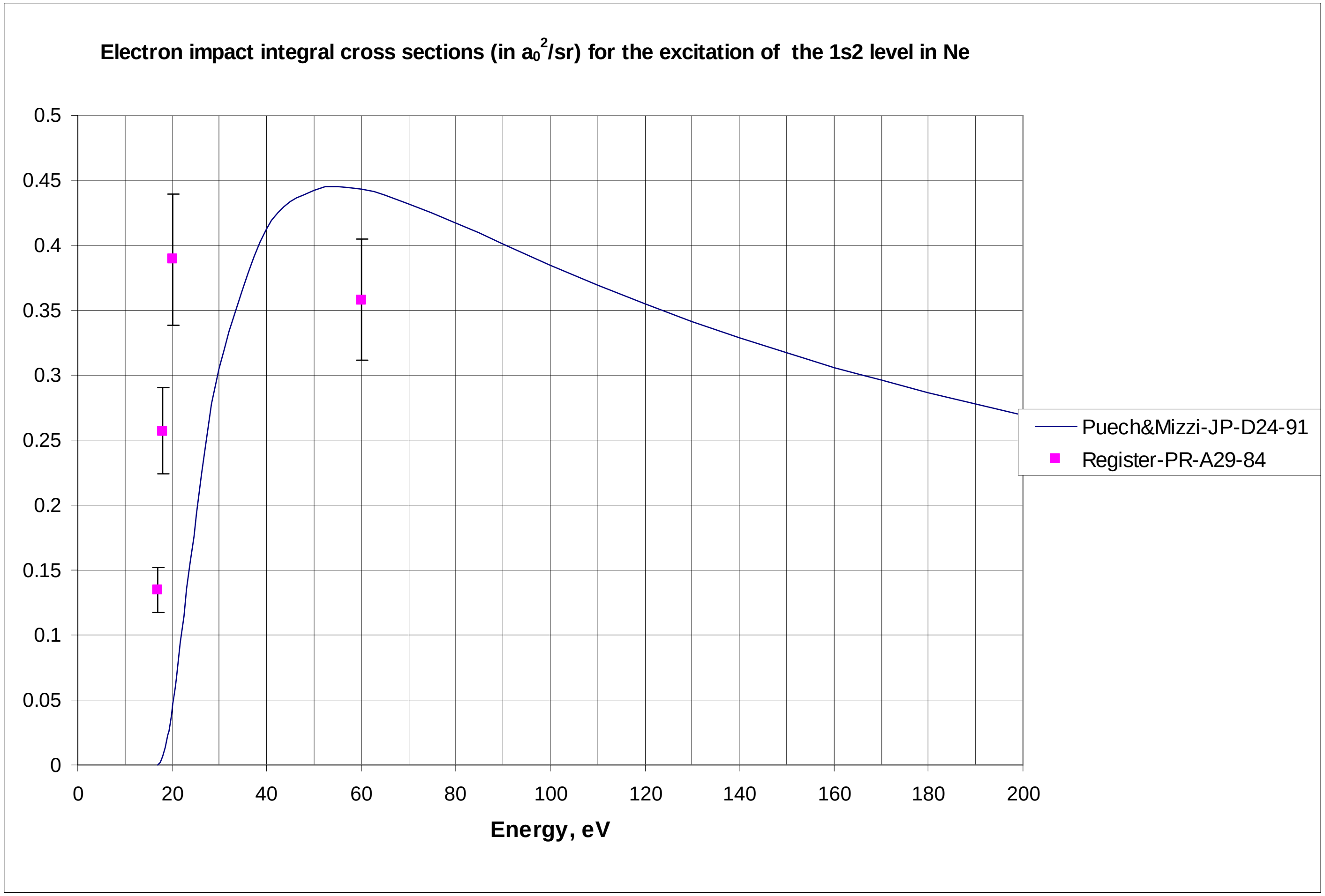

Demonstrates magnitude of disparity possible among similar data sets

Problems - 3

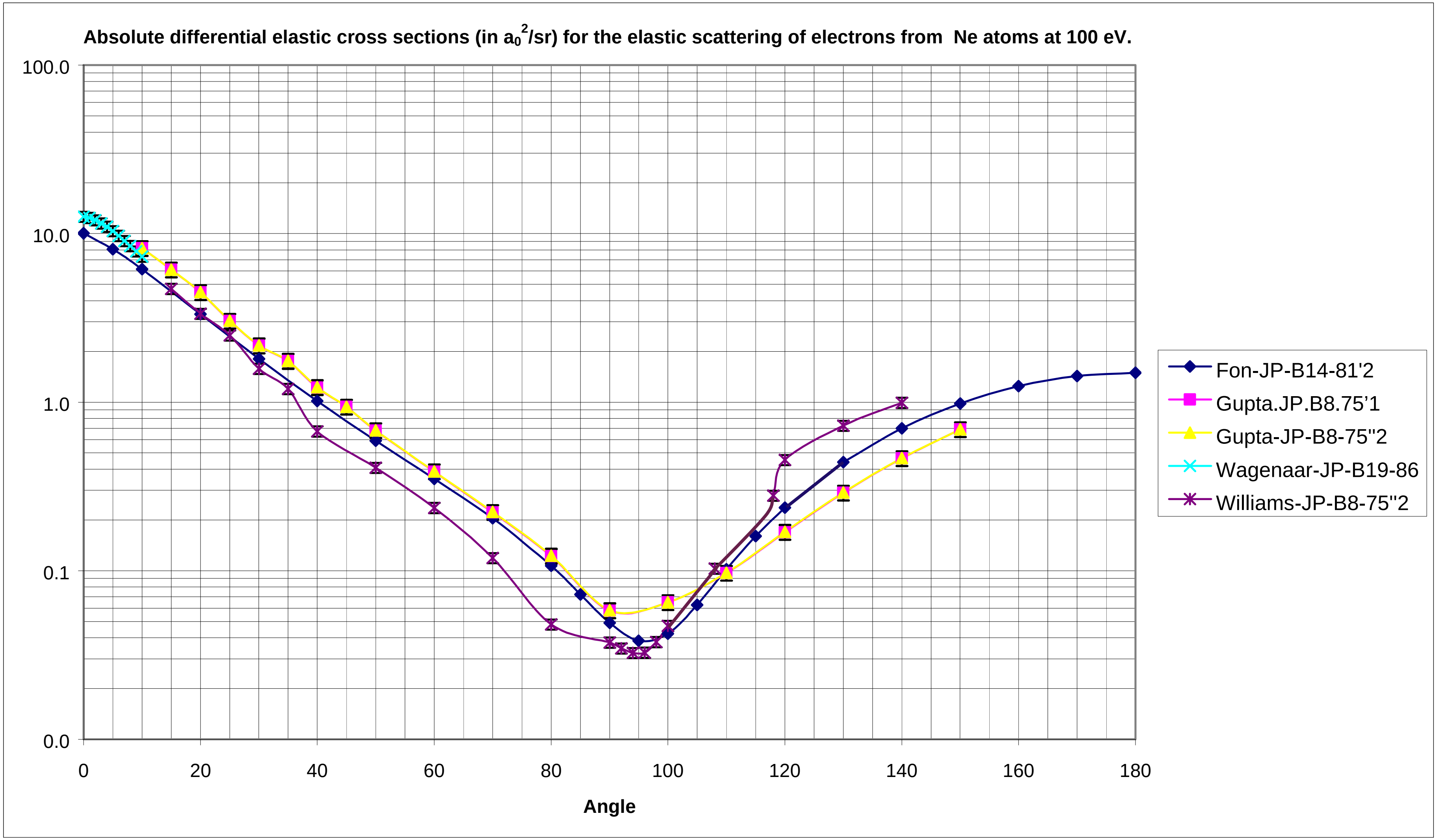

A chart demonstrating a typical comparison of similar data sets from different sources

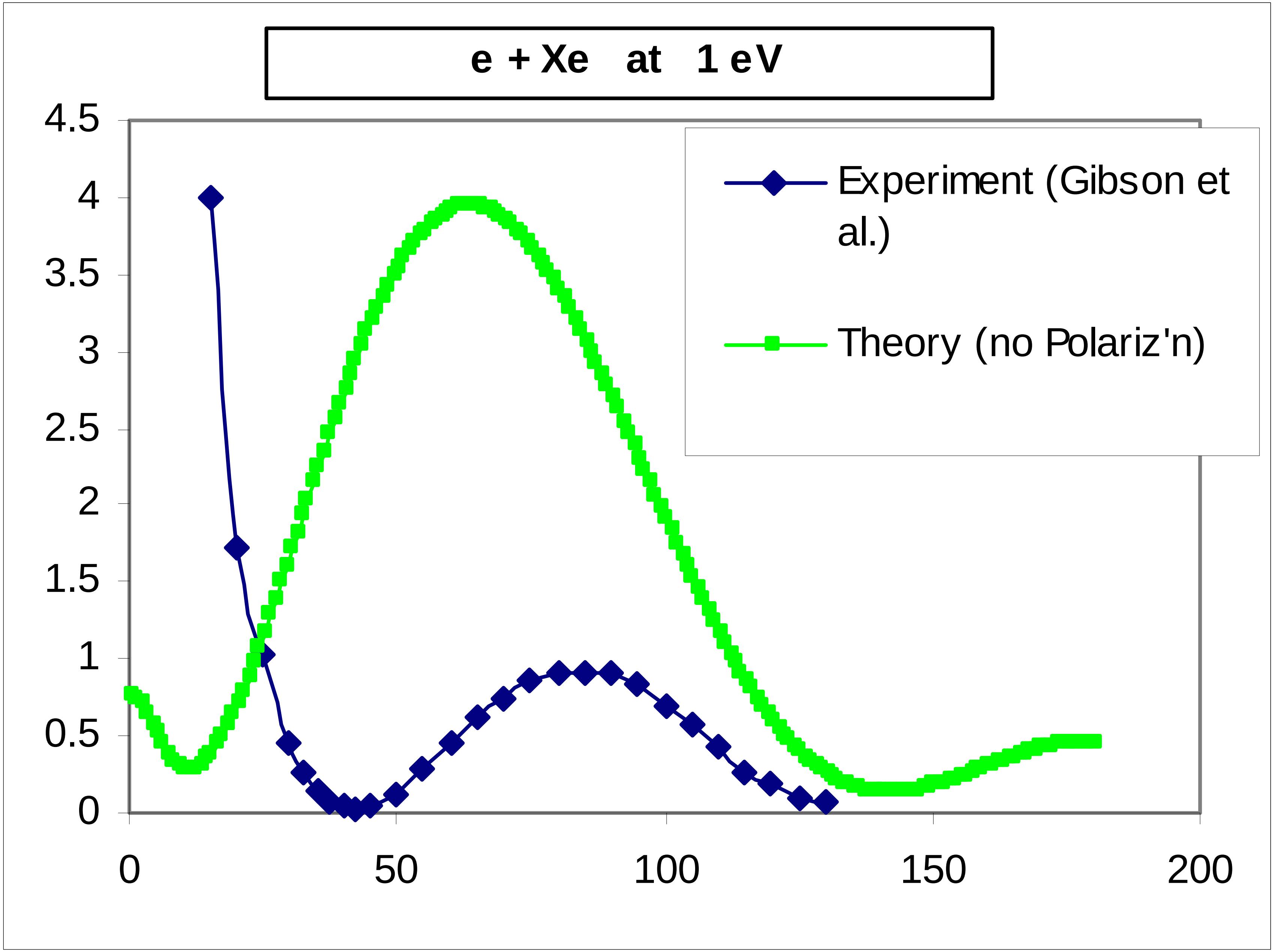
e + Xe at 1 eV
4.5
4
3.5
3
2.5
2
1.5
1
0.5
0
0
50
100
150
200
Experiment (Gibson et al.)
Theory (no Polariz'n)

Fits of differential cross sections

- The experimental cross sections were fitted to the form:

$$\frac{d\sigma}{d\Omega}(\theta) = A\exp(-\theta / B) + C\exp[-(\pi - \theta)^4 / D]$$

$$+\sum_{l=0}^{4-10} a_l P_l(\cos\theta)$$

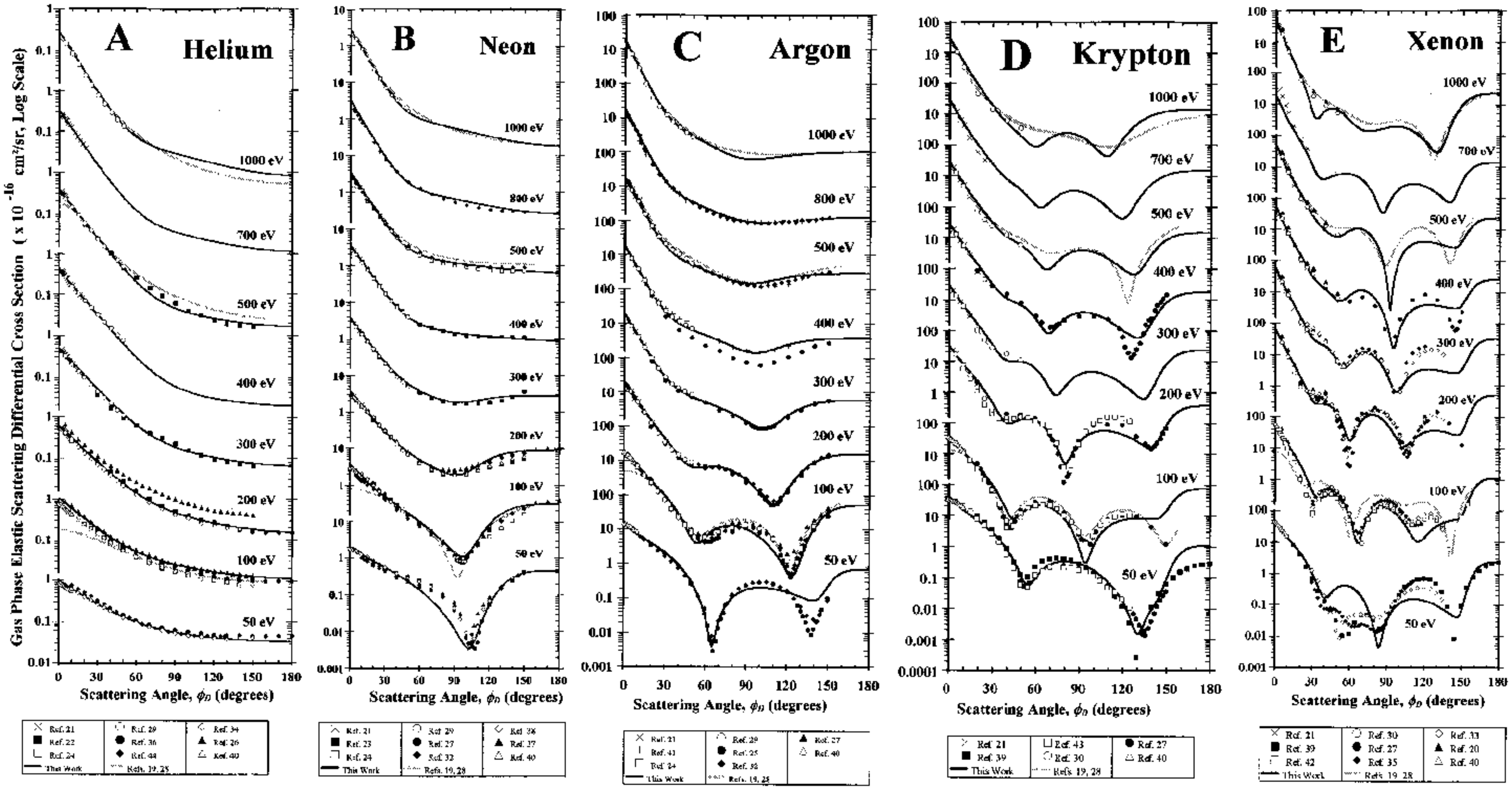

Figure 5. Logarithmic plots of experimental elastic differential cross sections for the rare gases. Gas phase measurements (individual points) are compared with the present description (heavy solid lines) and previous theoretical treatments (fine lines). References are shown in the legend below each plot. The logarithmic format allows the large-angle portions of the distributions to be seen more clearly by exaggerating the low intensities.

Our Objective: A **simple** and **dependable** calculation for **elastic scattering cross sections** of electrons from atoms and ions for gaseous discharge studies.

Reasons:

Realistic calculations of gas discharges require

- **total**
- **momentum transfer**
- **angle-differential cross sections**

(to account for anisotropic scattering events)

The vast majority of such calculations assume isotropic elastic scattering

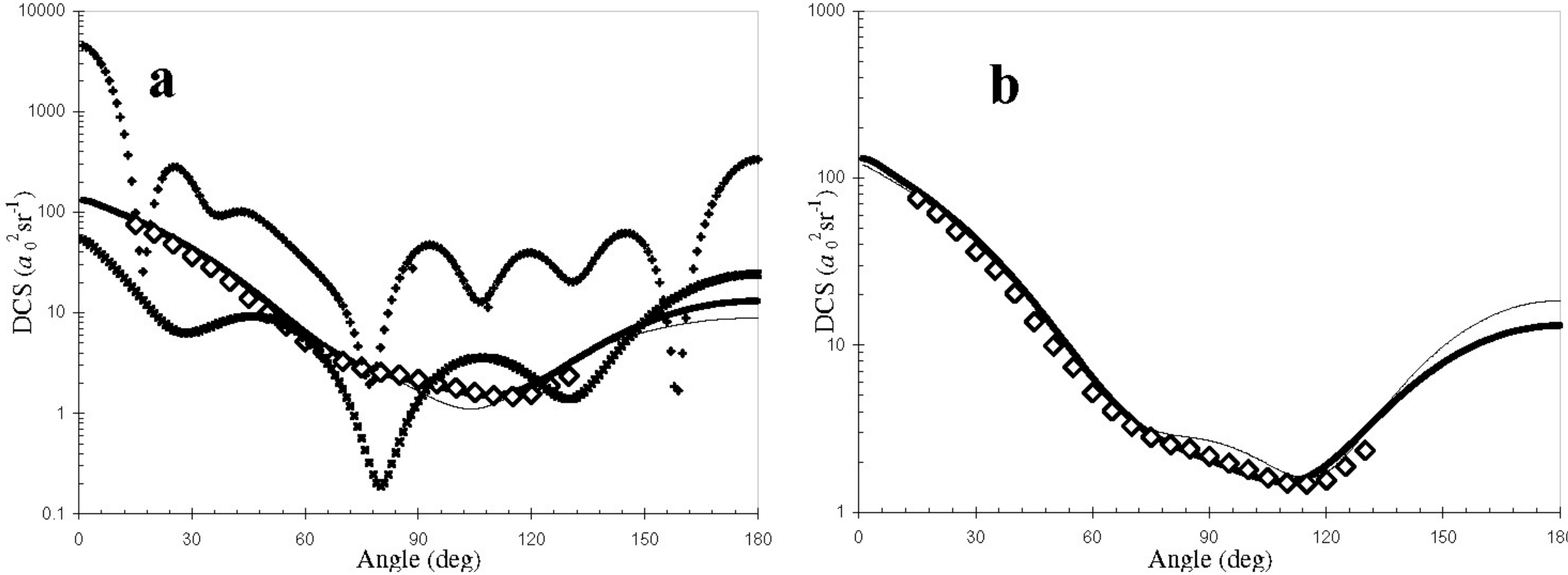

FIG. 2: Studying the effect of different choices of central atomic and exchange potentials on present DCS values for xenon at 10 eV: **a**) Comparison with experimental values while the central atomic potential varies, but Exchange (SC) and polarization (Buckingham-type II) potential remain unchanged: ◊, Gibson *et al.* [40]; thick solid line, DS potential [8]; thin solid line, Salvat *et al.* potential [7]; +, HF potential; ×, Green *et al.* potential [5, 6]. **b**) Comparison with experimental values while the exchange potential varies, but Central atomic (DS) and polarization (Buckingham-type II) potential remain unchanged: ◊, Gibson *et al.* [40]; thick solid line, SC exchange potential; thin solid line, FEG exchange potential.

General theoretical expression

$$\frac{d\sigma}{d\Omega}(\theta) = \left| f_c(\theta) + f_{nc}(\theta) \right|^2$$

$$f_c = \frac{-\alpha \exp(2i\sigma_0)}{2\mu v \sin^2(\theta/2)} \exp[-i\alpha \log(\sin^2(\theta/2))]$$

$$\alpha = -q/v \qquad \sigma_l = \arg(\Gamma(l+1+i\alpha))$$

$$f_{nc} = \frac{1}{2ik} \sum_{l=0}^{l_{\max}} (2l+1) \exp(2i\sigma_l)(\exp(2i\delta_l)-1) P_l(\cos\theta)$$

General theoretical expressions - neutral targets

Scattering amplitudes

$$f(\theta)=\frac{1}{k}\sum_{l=0}^{\infty}\left[(l+1)e^{i\delta_l^+(k)}\sin\delta_l^+(k)+le^{i\delta_l^-(k)}\sin\delta_l^-(k)\right]P_l(\cos\theta)$$

$$g(\theta)=\frac{1}{k}\sum_{l=0}^{\infty}\left[e^{i\delta_l^-(k)}\sin\delta_l^-(k)-e^{i\delta_l^+(k)}\sin\delta_l^+(k)\right]P_l^1(\cos\theta)$$

Differential elastic cross section

$$\frac{d\sigma}{d\Omega}(\theta,k)=\left|f(\theta)\right|^2+\left|g(\theta)\right|^2$$

Total elastic cross section

$$\sigma(k)=\frac{4\pi}{k^2}\sum_{l}\left[\left(l+1\right)\sin^2\delta_l^+(k)+l\sin^2\delta_l^-(k)\right]$$

Momentum transfer cross section

$$\sigma_m(k)=\frac{4\pi}{k^2}\sum_{l=0}^{\infty}\left\{\begin{array}{l}\frac{(l+1)(l+2)}{2l+3}\sin^2\left(\delta_l^+(k)-\delta_{l+1}^+(k)\right)\\+\frac{l(l+1)}{2l+1}\sin^2\left(\delta_l^-(k)-\delta_{l+1}^-(k)\right)\\+\frac{(l+1)}{(2l+1)(2l+3)}\sin^2\left(\delta_l^+(k)-\delta_{l+1}^-(k)\right)\end{array}\right\}$$

Sherman function

$$\mathrm{S}(\theta,k)=i\frac{f(\theta)g^*(\theta)-f^*(\theta)g(\theta)}{\left|f(\theta)\right|^2+\left|g(\theta)\right|^2}$$

Approximations

Atomic potential

Central Dirac-Slater potential

Electron exchange

Local approximation of Furness and McCarthy's [JPB **6, 2280 (1973)]**

$$V_{\mathrm{exch}}(r) = \frac{1}{2}\left[\left|E - V_s(r)\right| - \left(\left|E - V_s(r)\right|^2 + 4\pi\rho(r)\right)^{1/2}\right]$$

$$V_s(r) = -\frac{2}{r}\left[Z - Y(r)\right]; \quad Y(r) = \sum_{i=1}^{N}\left\{\int_0^r u_i^2(r')dr' + r\int_r^\infty [u_i^2(r')/r']dr'\right\}.$$

Core polarization effects

$$V_{\mathrm{pol}}(r) = -\frac{\alpha_d}{2(r^2 + d^2)^2} \qquad d = \langle r \rangle_{np} + \frac{1}{3}\ln(E/\mathrm{Ry})$$

Some examples/results

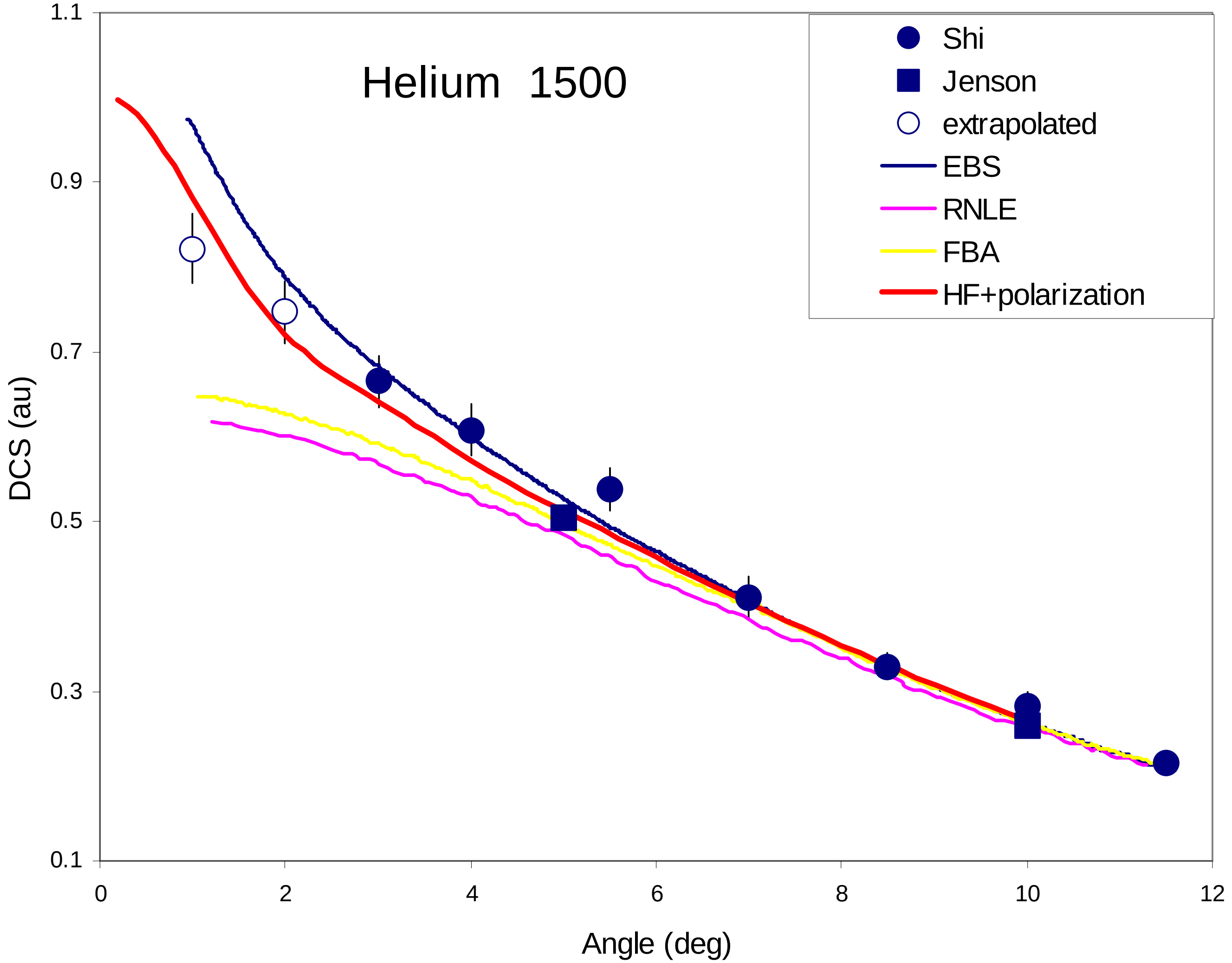

Griffin and Pindzola, Phys. Rev A **53**, 1915 (1996)

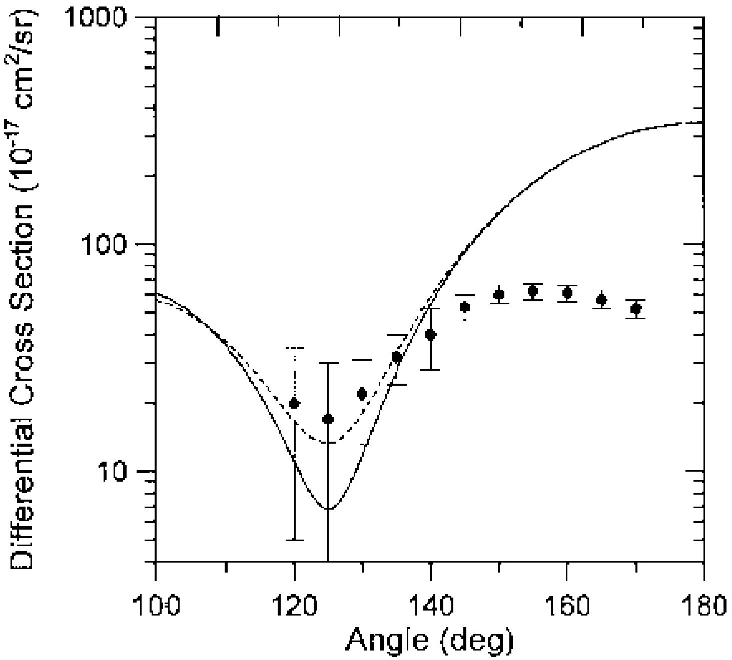

FIG. 1. Angular differential cross section for elastic scattering in Ar^+ at 3.3 eV. Solid curve: from a 17-state R-matrix calculation including polarized pseudostates; dashed curve: from a 17-state calculation convoluted over energy and angle using the energy and angular widths given in Ref. [1]; experimental points are from Ref. [1].

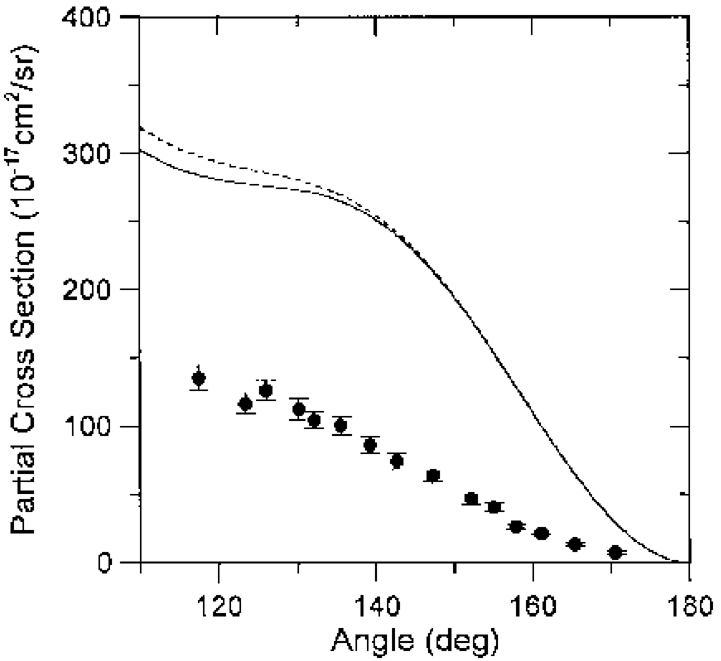

FIG. 2. Partial differential cross section for elastic scattering in Ar^+ at 3.3 eV from an initial angle through 180°, as a function of the initial angle. Solid curve: from 17-state R-matrix calculation; dashed curve: from a 17-state calculation convoluted over energy and angle before integration over the angle; experimental points: from Ref. [1].

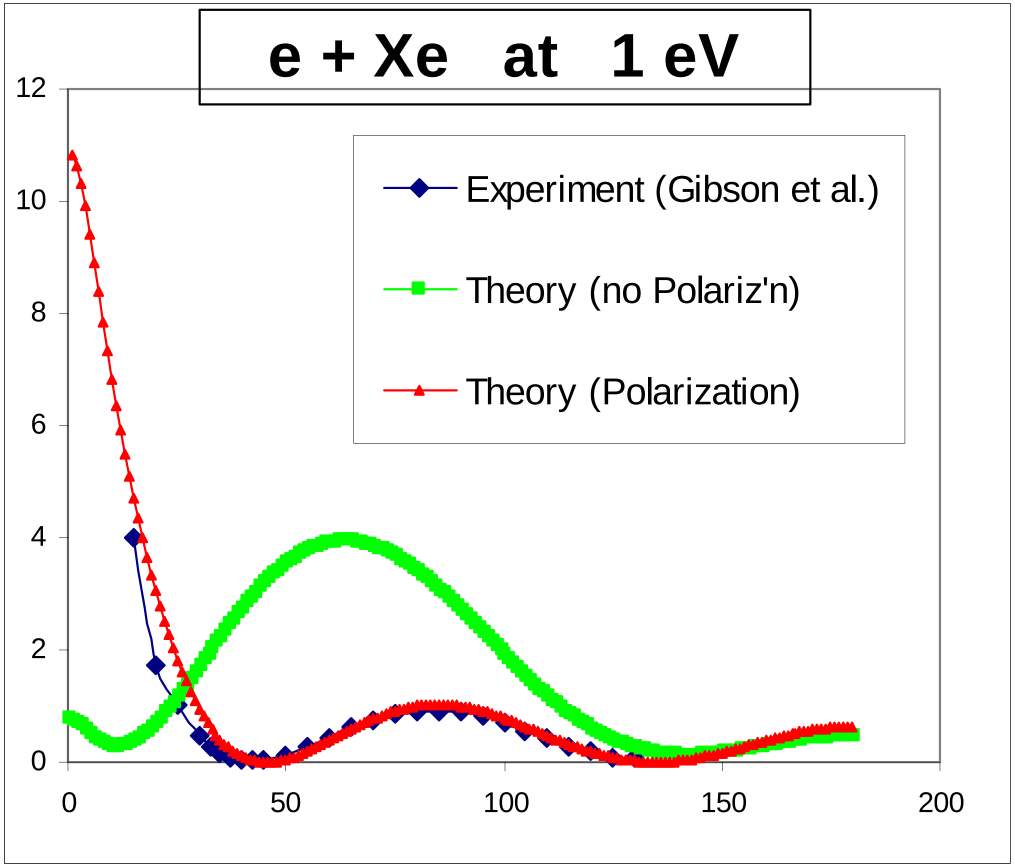

e + Xe at 1 eV
12
10
8
6
4
2
0
0
50
100
150
200
Experiment (Gibson et al.)
Theory (no Polariz'n)
Theory (Polarization)

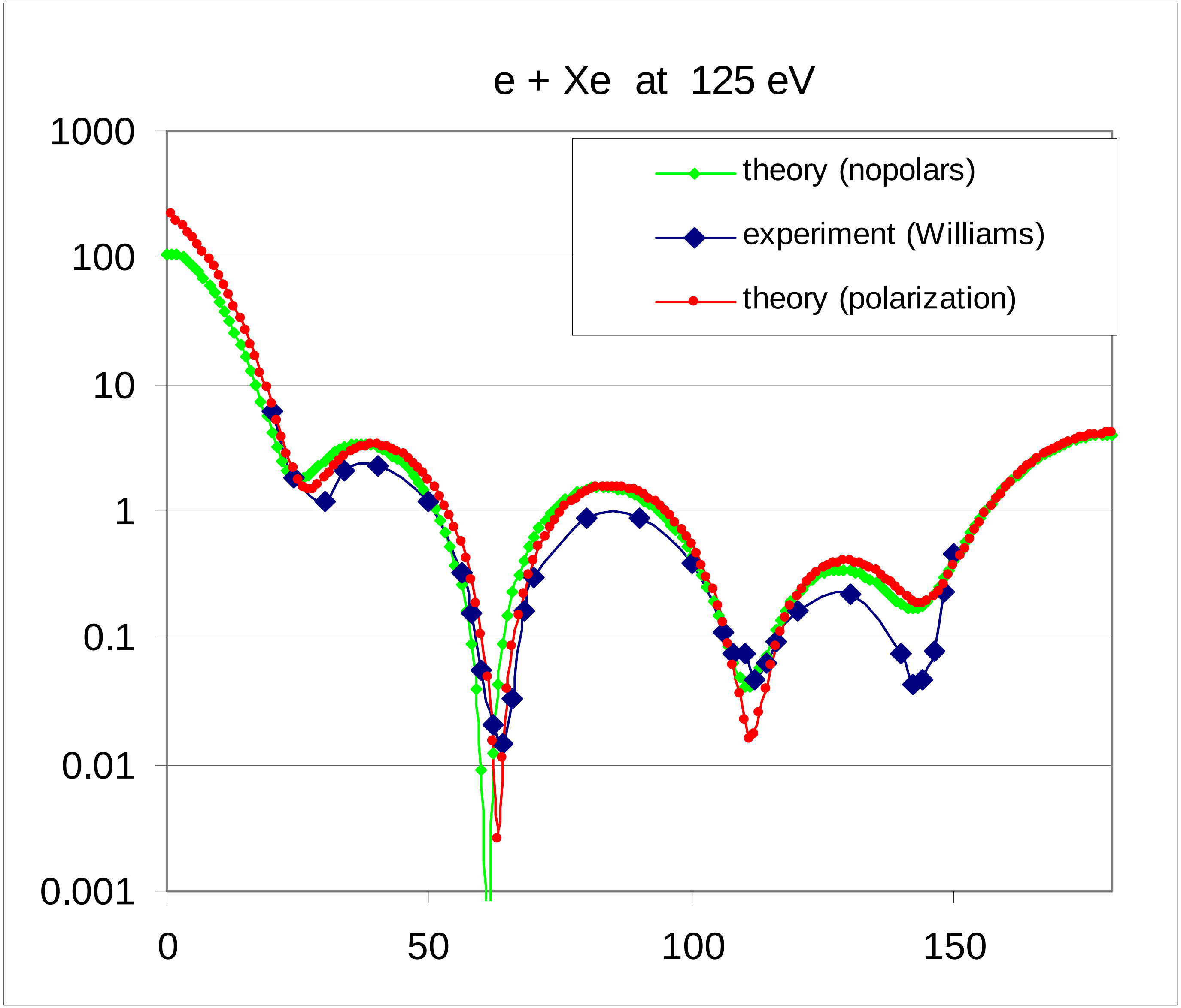
e + Xe at 125 eV
theory (nopolars)
experiment (Williams)
theory (polarization)
1000
100
10
1
0.1
0.01
0.001
0
50
100
150

Atoms studied completely

He Ne Ar Kr Xe

Sr Ba

Be Mg Ca

Cd Zn Hg

Parametric fitting of results

- Experimental data were fitted by varying the cutoff distance *d*.
- After the fit, the trend of the values of *d* was examined.
- We found:

for *Ne, Ar, Kr, Xe, Ba, Sr, Be, Mg, Ca, Zn, Cd, Hg*

$$d = \langle r \rangle_{np} + \frac{1}{3}\ln(E/\mathrm{Ry})$$

and a linear relationship for *He*,

$$d = 0.73 + 0.04(E/\mathrm{Ry})$$

He

Helium


1.5 eV
DCS (a.u.)
0
1
2
0
30
60
90
120
150
180
Angle
Brunger
Present

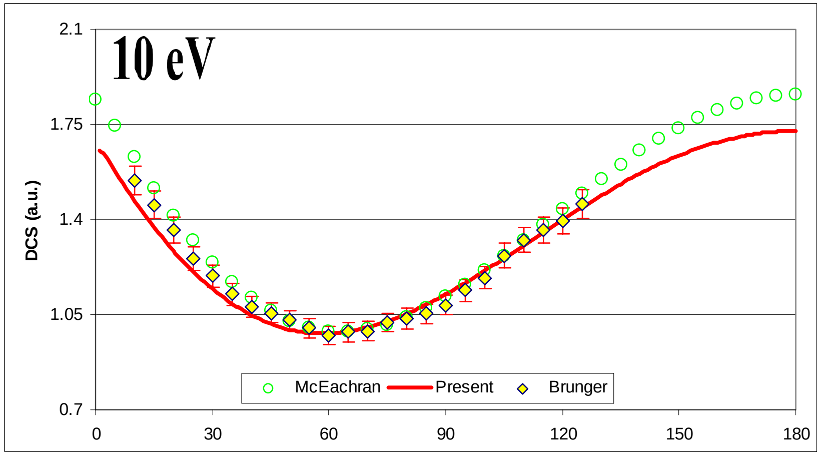
10 eV
DCS (a.u.)
0.7
1.05
1.4
1.75
2.1
0
30
60
90
120
150
180
McEachran
Present
Brunger

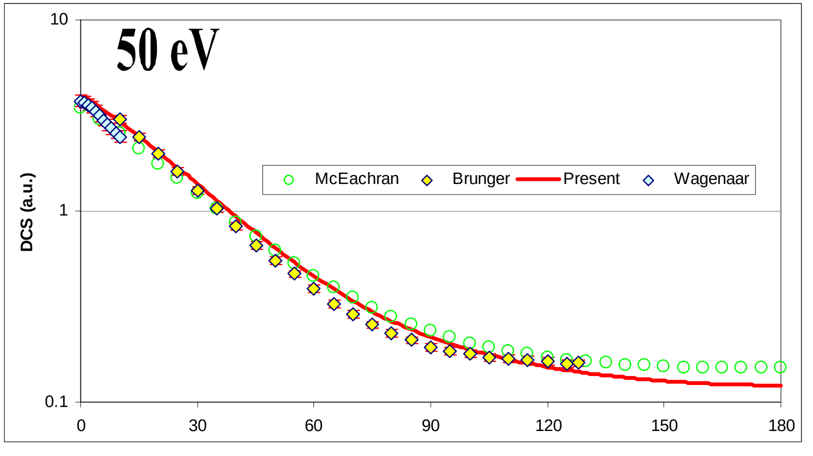
50 eV
DCS (a.u.)
0.1
1
10
0
30
60
90
120
150
180
McEachran
Brunger
Present
Wagenaar

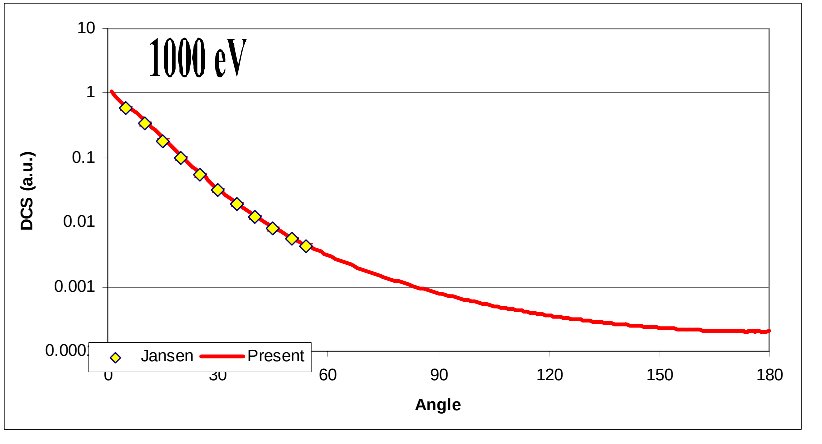
1000 eV
DCS (a.u.)
0.0001
0.001
0.01
0.1
1
10
0
30
60
90
120
150
180
Angle
Jansen
Present

Ne

Neon

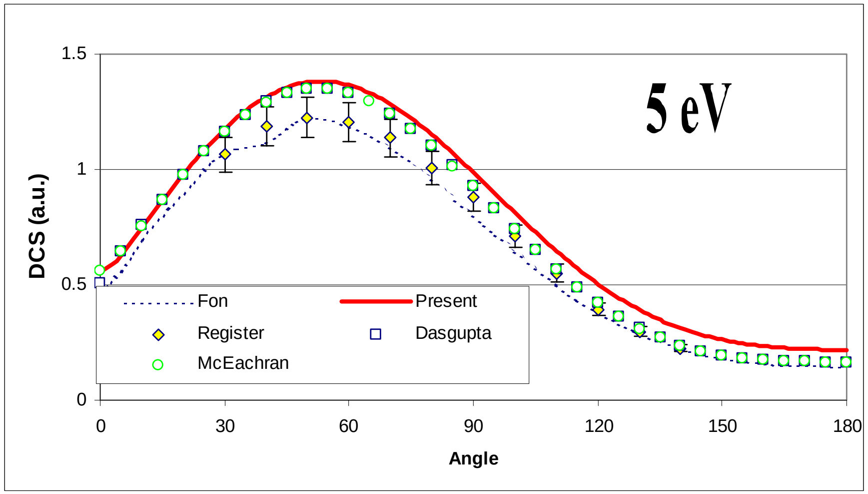

5 eV
DCS (a.u.)
Angle
0
0.5
1
1.5
0
30
60
90
120
150
180
Fon
Present
Register
Dasgupta
McEachran

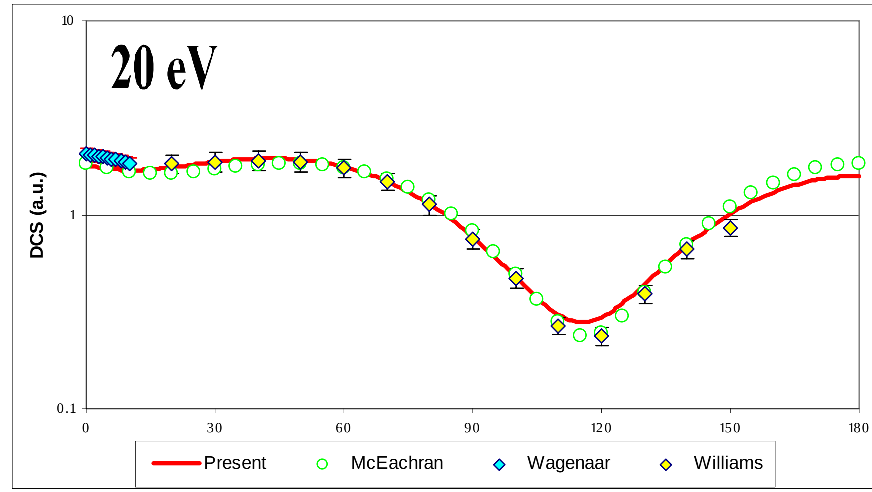

20 eV
DCS (a.u.)
0.1
1
10
0
30
60
90
120
150
180
Present
McEachran
Wagenaar
Williams

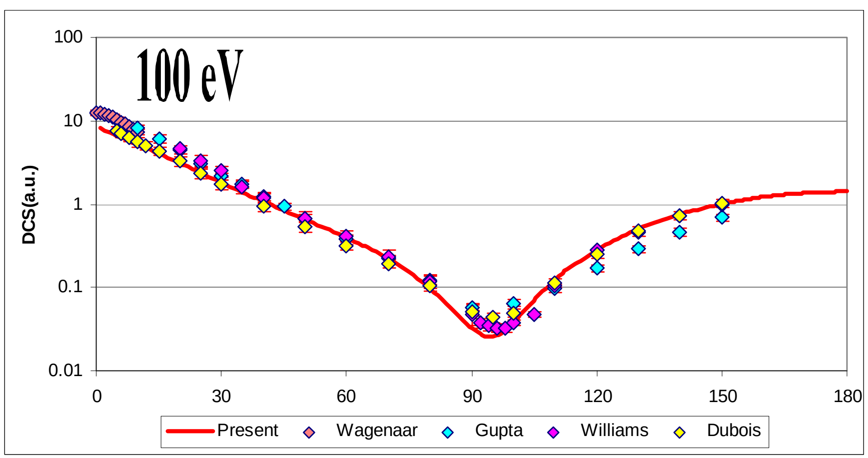

100 eV
DCS(a.u.)
0.01
0.1
1
10
100
0
30
60
90
120
150
180
Present
Wagenaar
Gupta
Williams
Dubois

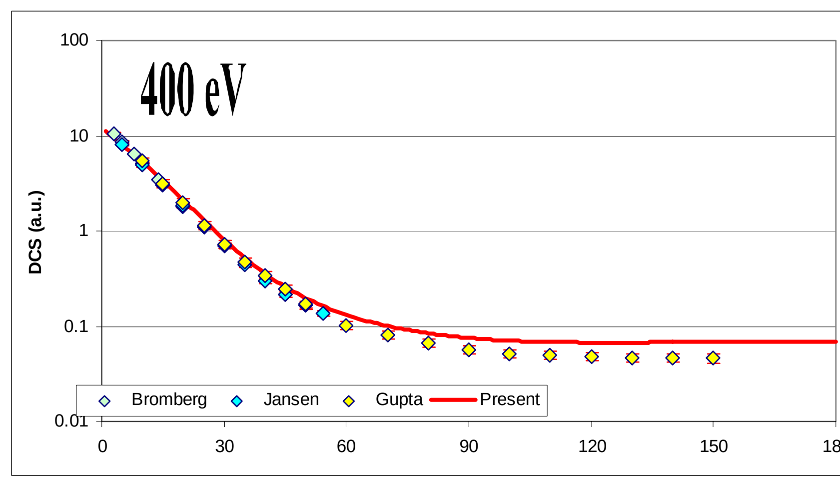

400 eV
DCS (a.u.)
0.01
0.1
1
10
100
0
30
60
90
120
150
180
Bromberg
Jansen
Gupta
Present

Ar

Argon

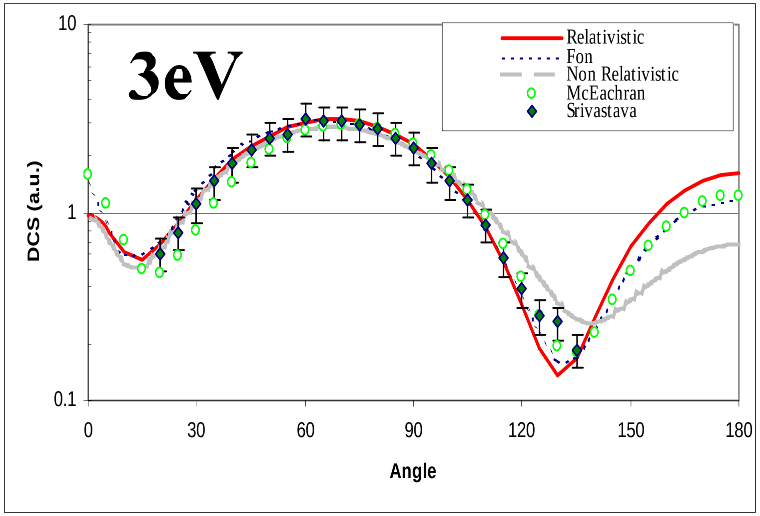
3eV
Relativistic
Fon
Non Relativistic
McEachran
Srivastava
DCS (a.u.)
Angle
10
1
0.1
0
30
60
90
120
150
180

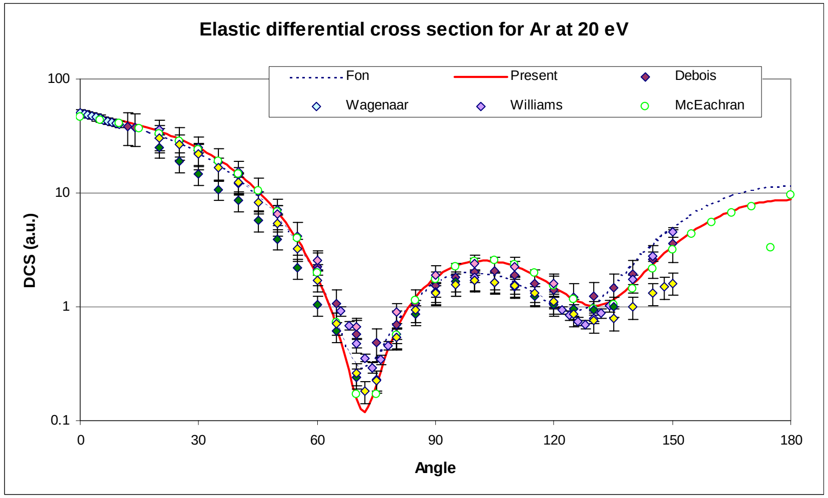
Elastic differential cross section for Ar at 20 eV
Fon
Present
Debois
Wagenaar
Williams
McEachran
DCS (a.u.)
Angle
100
10
1
0.1
0
30
60
90
120
150
180

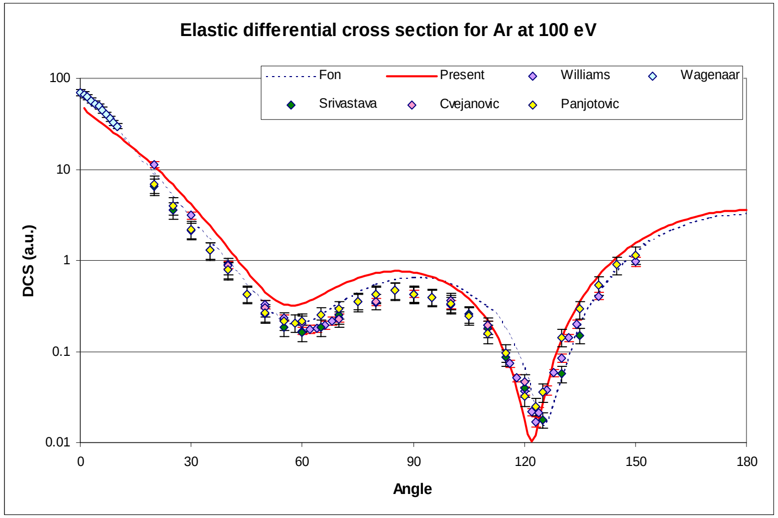
Elastic differential cross section for Ar at 100 eV
Fon
Present
Williams
Wagenaar
Srivastava
Cvejanovic
Panjotovic
DCS (a.u.)
Angle
100
10
1
0.1
0.01
0
30
60
90
120
150
180

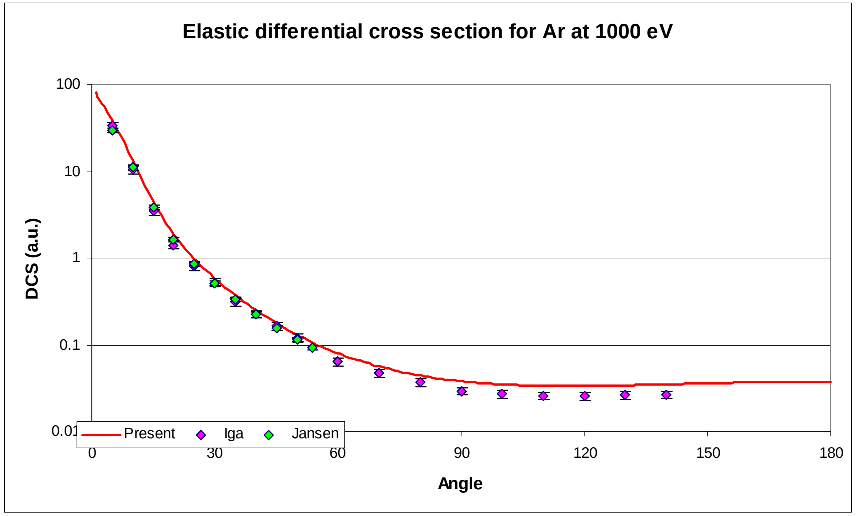
Elastic differential cross section for Ar at 1000 eV
Present
Iga
Jansen
DCS (a.u.)
Angle
100
10
1
0.1
0.01
0
30
60
90
120
150
180

Kr

Krypton

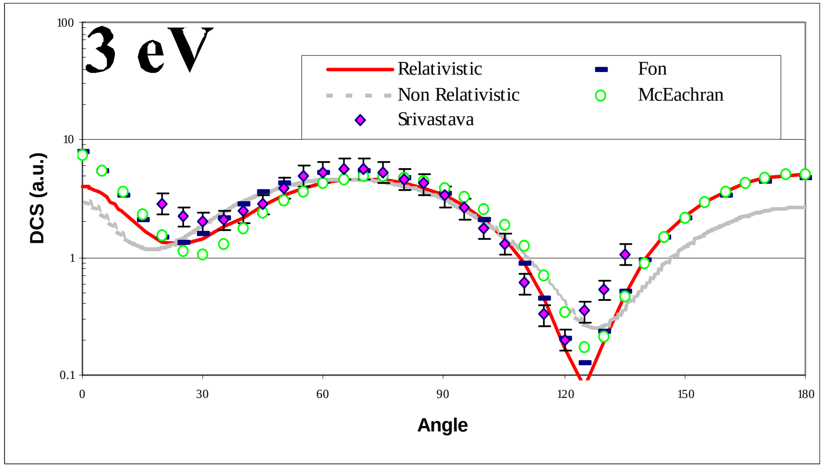

3 eV
Relativistic
Non Relativistic
Srivastava
Fon
McEachran
DCS (a.u.)
Angle

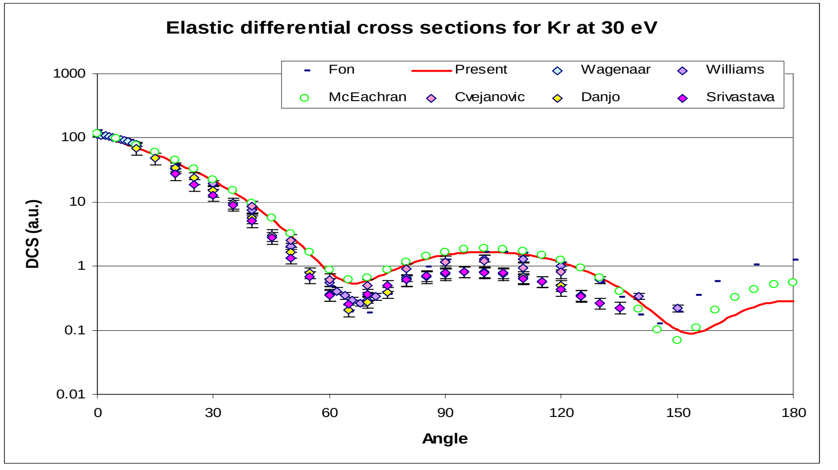

Elastic differential cross sections for Kr at 30 eV
Fon
Present
Wagenaar
Williams
McEachran
Cvejanovic
Danjo
Srivastava
DCS (a.u.)
Angle

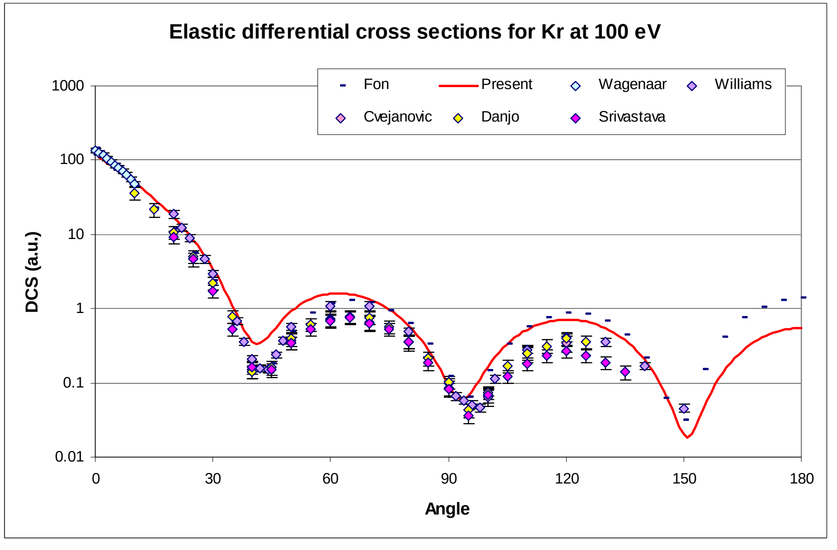

Elastic differential cross sections for Kr at 100 eV
Fon
Present
Wagenaar
Williams
Cvejanovic
Danjo
Srivastava
DCS (a.u.)
Angle

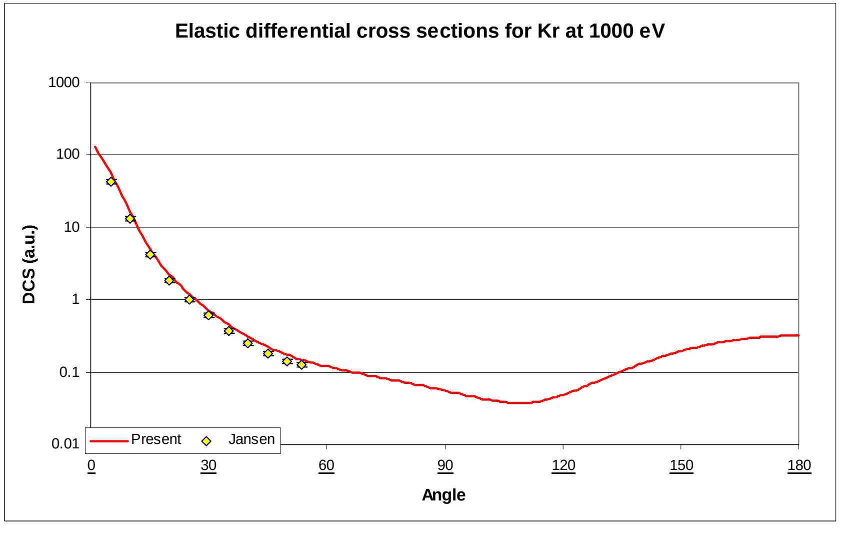

Elastic differential cross sections for Kr at 1000 eV
Present
Jansen
DCS (a.u.)
Angle

Xe

Xenon

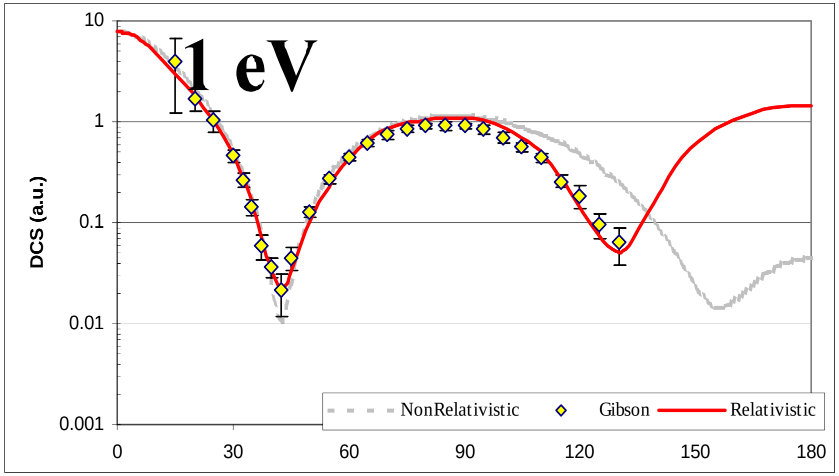
1 eV
DCS (a.u.)
10
1
0.1
0.01
0.001
0
30
60
90
120
150
180
NonRelativistic
Gibson
Relativistic

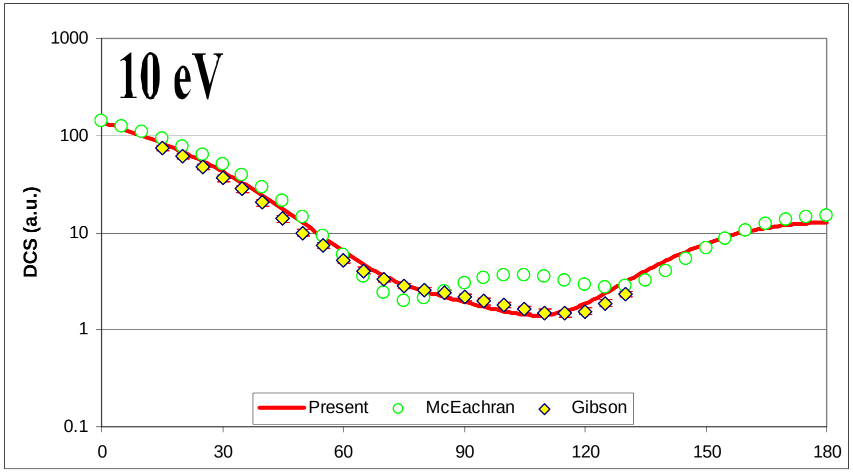
10 eV
DCS (a.u.)
1000
100
10
1
0.1
0
30
60
90
120
150
180
Present
McEachran
Gibson

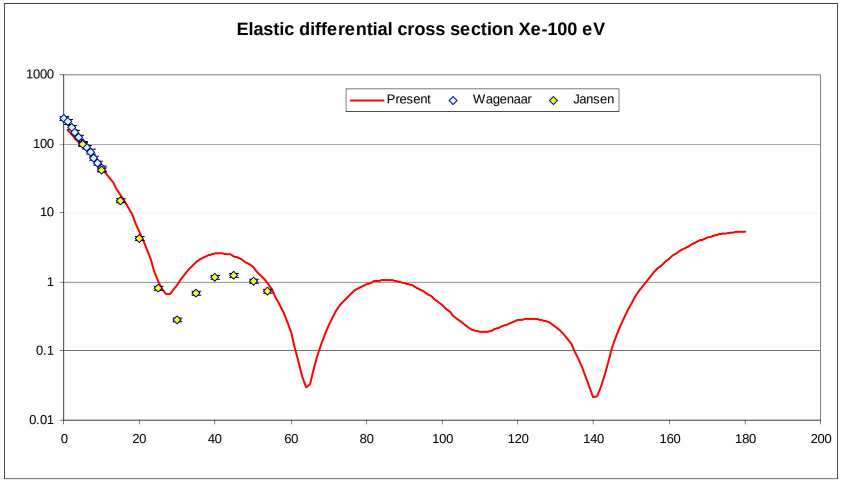
Elastic differential cross section Xe-100 eV
1000
100
10
1
0.1
0.01
0
20
40
60
80
100
120
140
160
180
200
Present
Wagenaar
Jansen

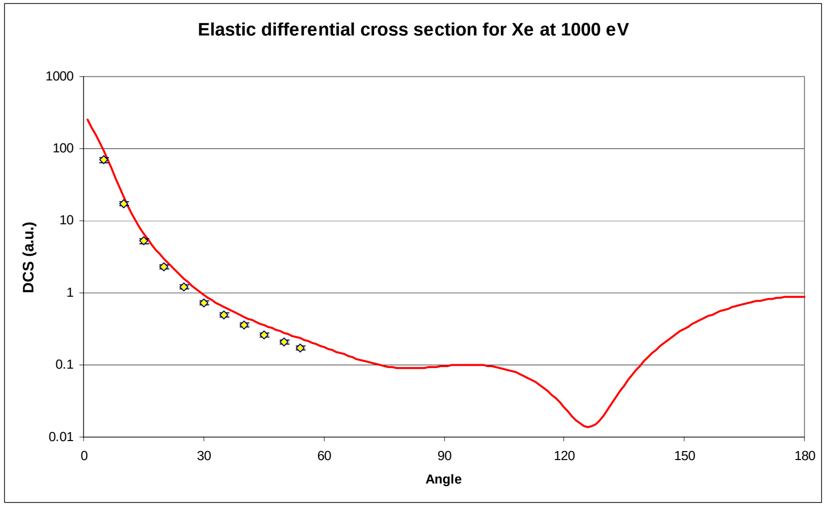
Elastic differential cross section for Xe at 1000 eV
DCS (a.u.)
1000
100
10
1
0.1
0.01
0
30
60
90
120
150
180
Angle

Ba

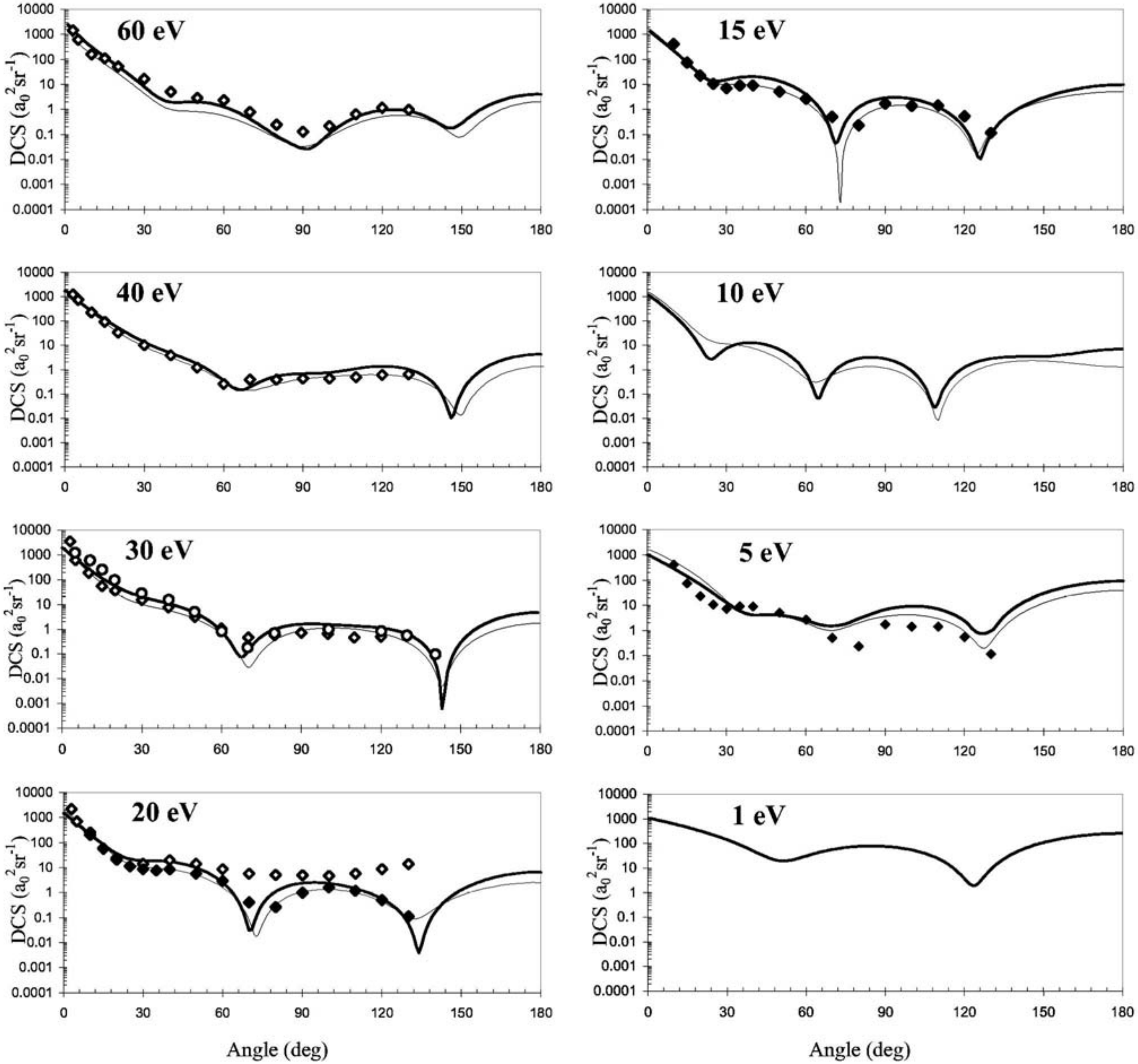

FIG. 2. Differential cross sections for elastic electron scattering by Ba from 1 to 60 eV: thick solid line, present work; thin solid line, CCC115 calculations of Fursa and Bray [22]. Experimental data: ◇, Jensen *et al.* [13]; ○, Trajmar [17]; ◆, Wang *et al.* [14].

Sr/Ba

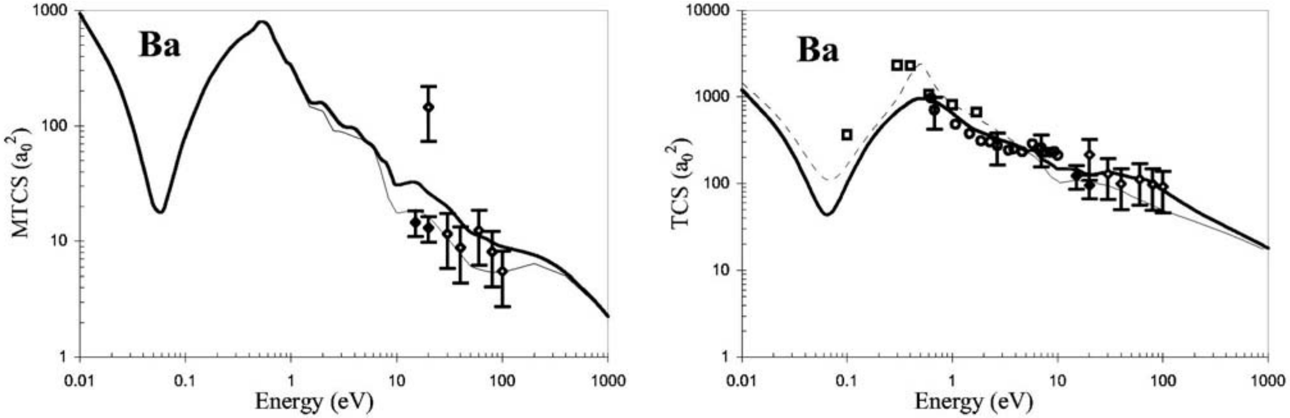

FIG. 7. Momentum transfer and total cross sections for elastic electron scattering from barium: thick solid line, present work. Experimental data: ○, Romanyuk *et al.* [5]; ◇, Jensen *et al.* [13]; ◆, Wang *et al.* [14]; Other theoretical: thin solid line, Fursa *et al.* [23]; dotted line, Yuan and Zhang [10]; □, Kelemen *et al.* [20].

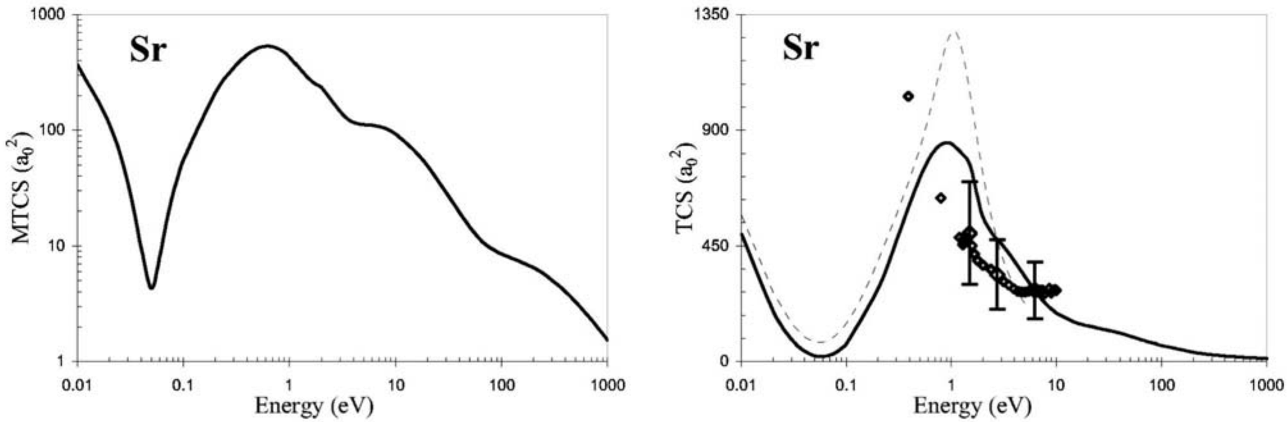

FIG. 8. Momentum transfer and total cross sections for elastic electron scattering from strontium: thick solid line, present work; ◇, experimental data of Romanyuk *et al.* [5]; Other theoretical: dotted line, Yuan and Zhang [10].

Be

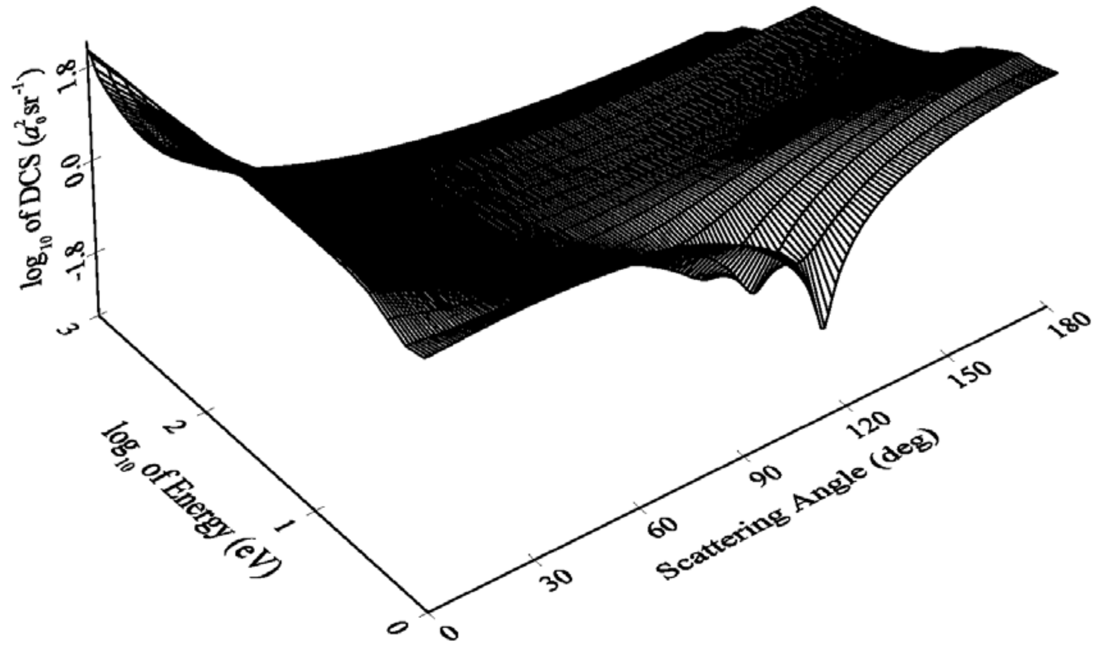

FIG. 3: a three-dimentional view of differential cross section for elastic electron scattering from beryllium.

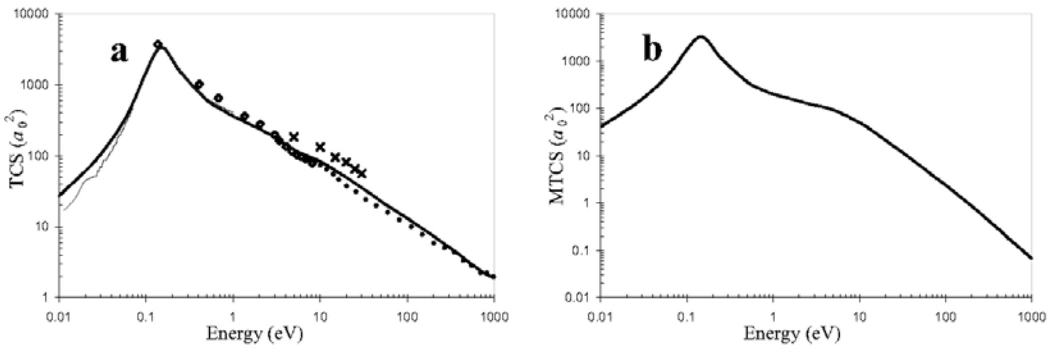

FIG. 4: Total (**a**) and momentum transfer (**b**) cross sections for elastic electron scattering from beryllium: thick solid line, present work; Other theoretical: thin solid line, Yuan and Zhang [11]; ×, Kaushik *et al.* [10]; ◊, Fabrikant [9]; •, Fursa and Bray[4, 5].

Mg

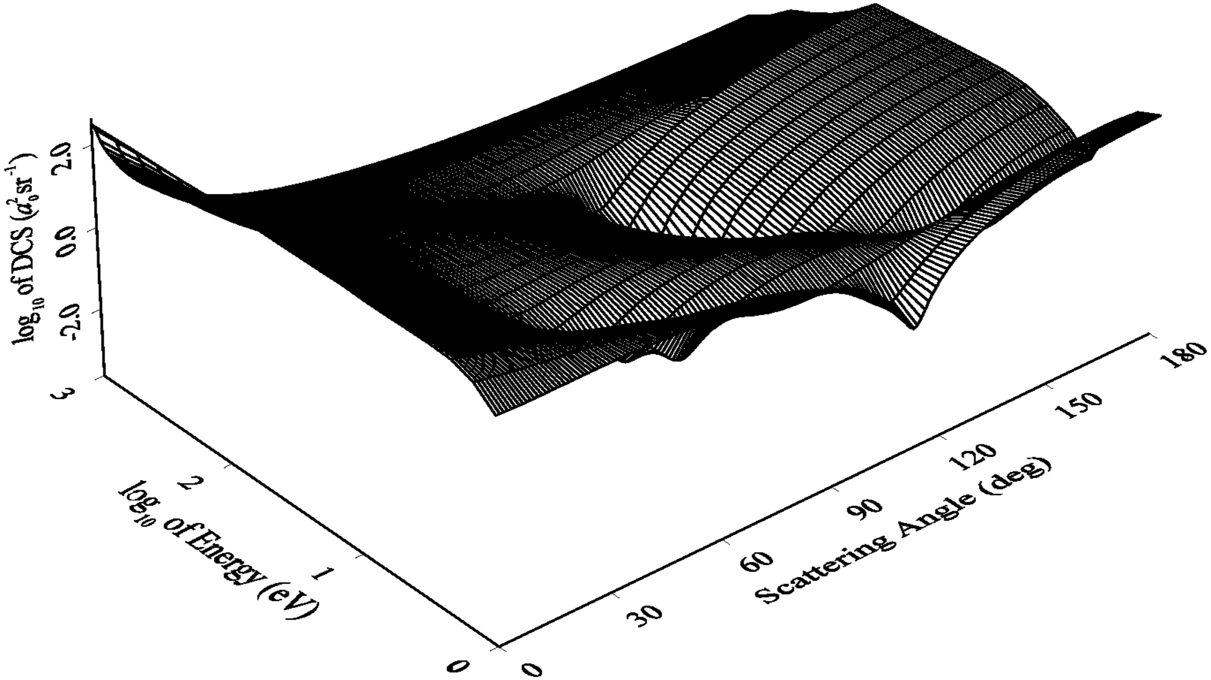

FIG. 7: a three-dimentional view of differential cross section for elastic electron scattering from magnesium.

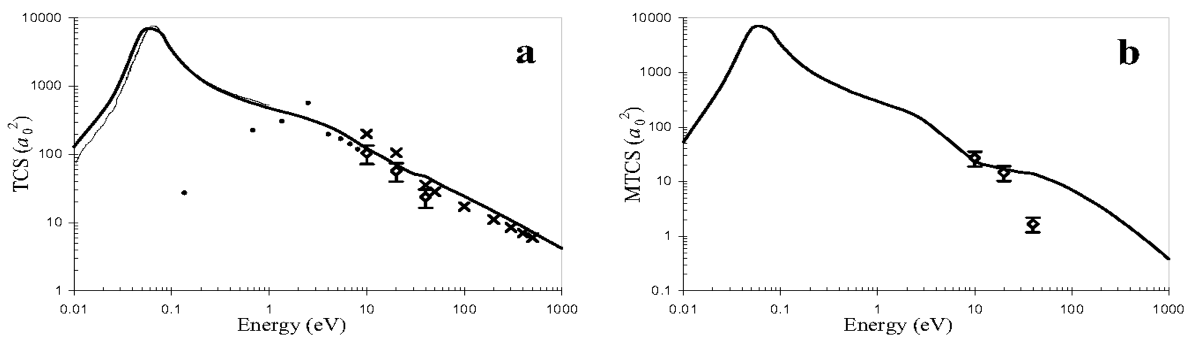

FIG. 8: Total (**a**) and momentum transfer (**b**) cross sections for elastic electron scattering from magnesium: thick solid line, present work; Experimental data: ◊, Williams and Trajmar [15]; Other theoretical: thin solid line, Yuan and Zhang [11]; ×, Khare *et al.* [20]; •, Fabrikant [9, 17].

Ca

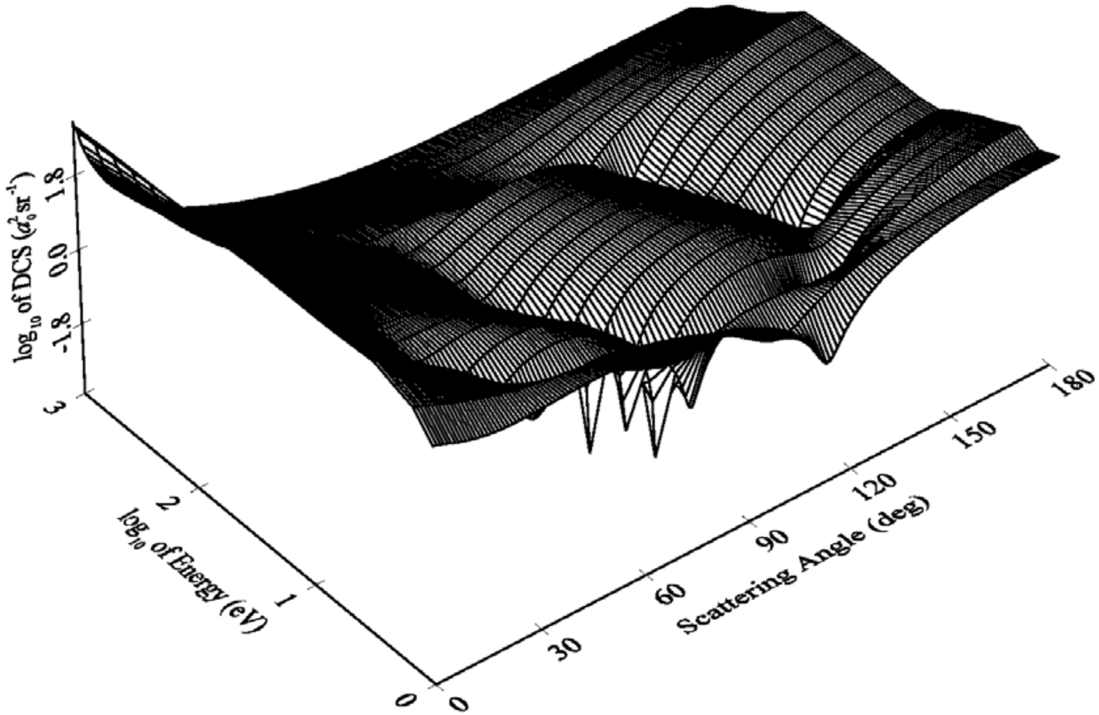

FIG. 11: a three-dimentional view of differential cross section for elastic electron scattering from calcium.

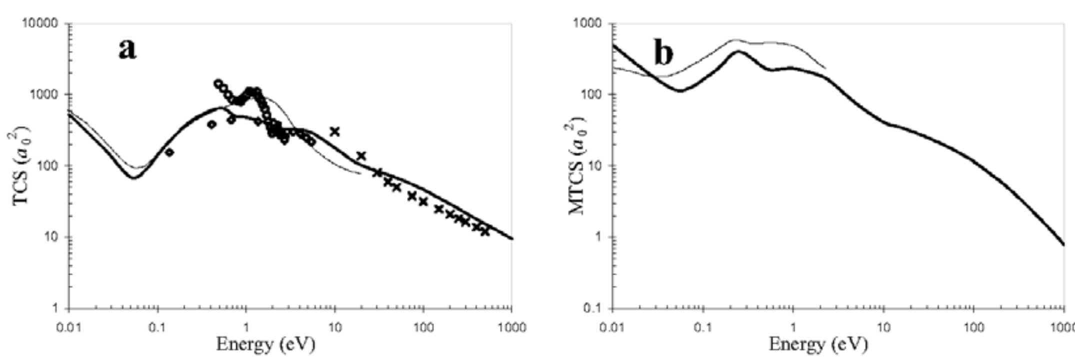

FIG. 12: Total (a) and momentum transfer (b) cross sections for elastic electron scattering from calcium: **Legend for TCS graph**: thick solid line, present work; Experimental data: ○, Romanyuk *et al.* [23]; Other theoretical: thin solid line, Yuan [26]; ◊, Fabrikant [9]; ×, Khare *et al.* [24]; **Legend for MTCS graph**: thick solid line, present work; Other theoretical: thin solid line, Cribakin *et al.* [25].

Zn

Zinc

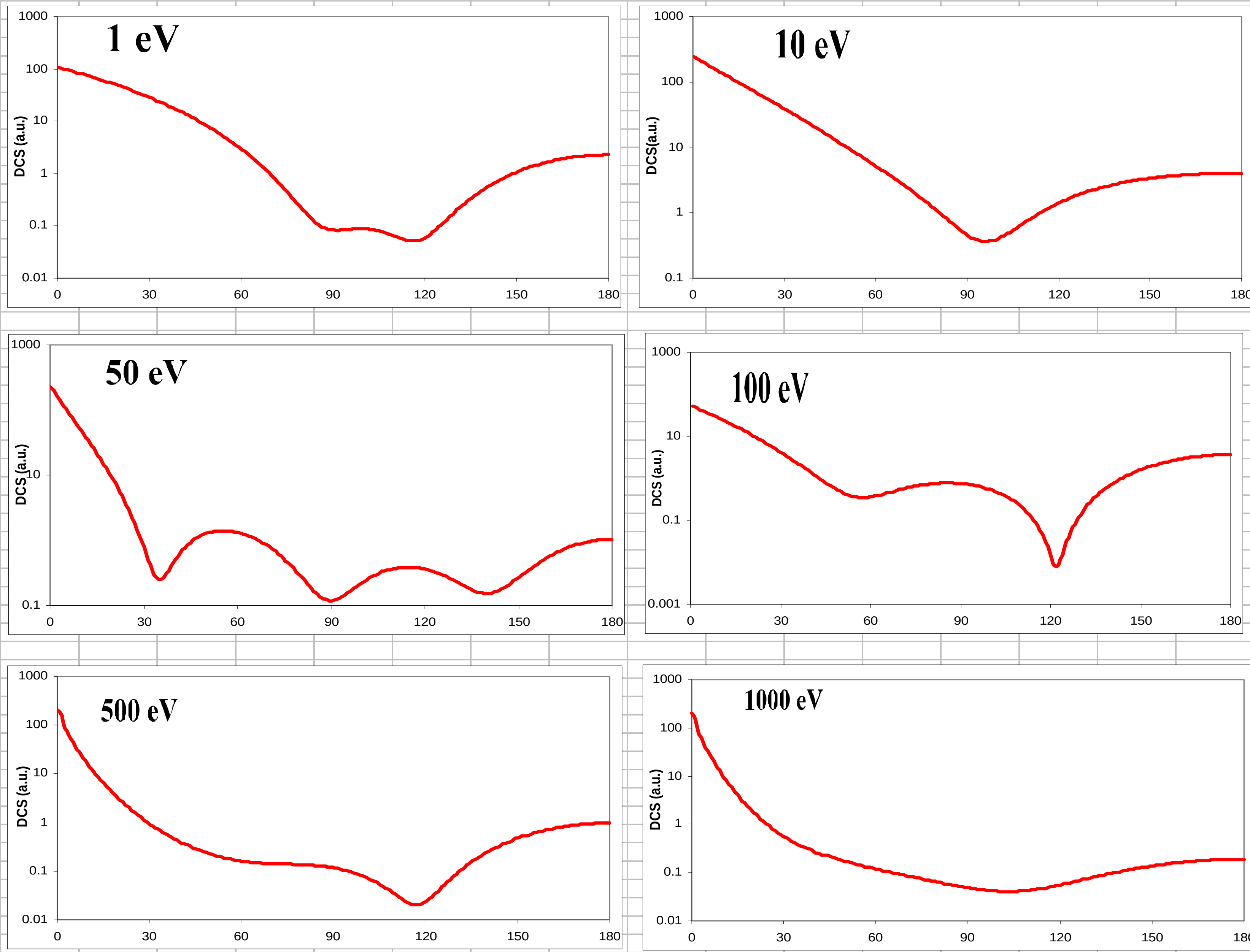
1 eV
10 eV
50 eV
100 eV
500 eV
1000 eV
DCS (a.u.)
DCS(a.u.)
1000
100
10
1
0.1
0.01
0.001
0
30
60
90
120
150
180

Cd

Cadmium

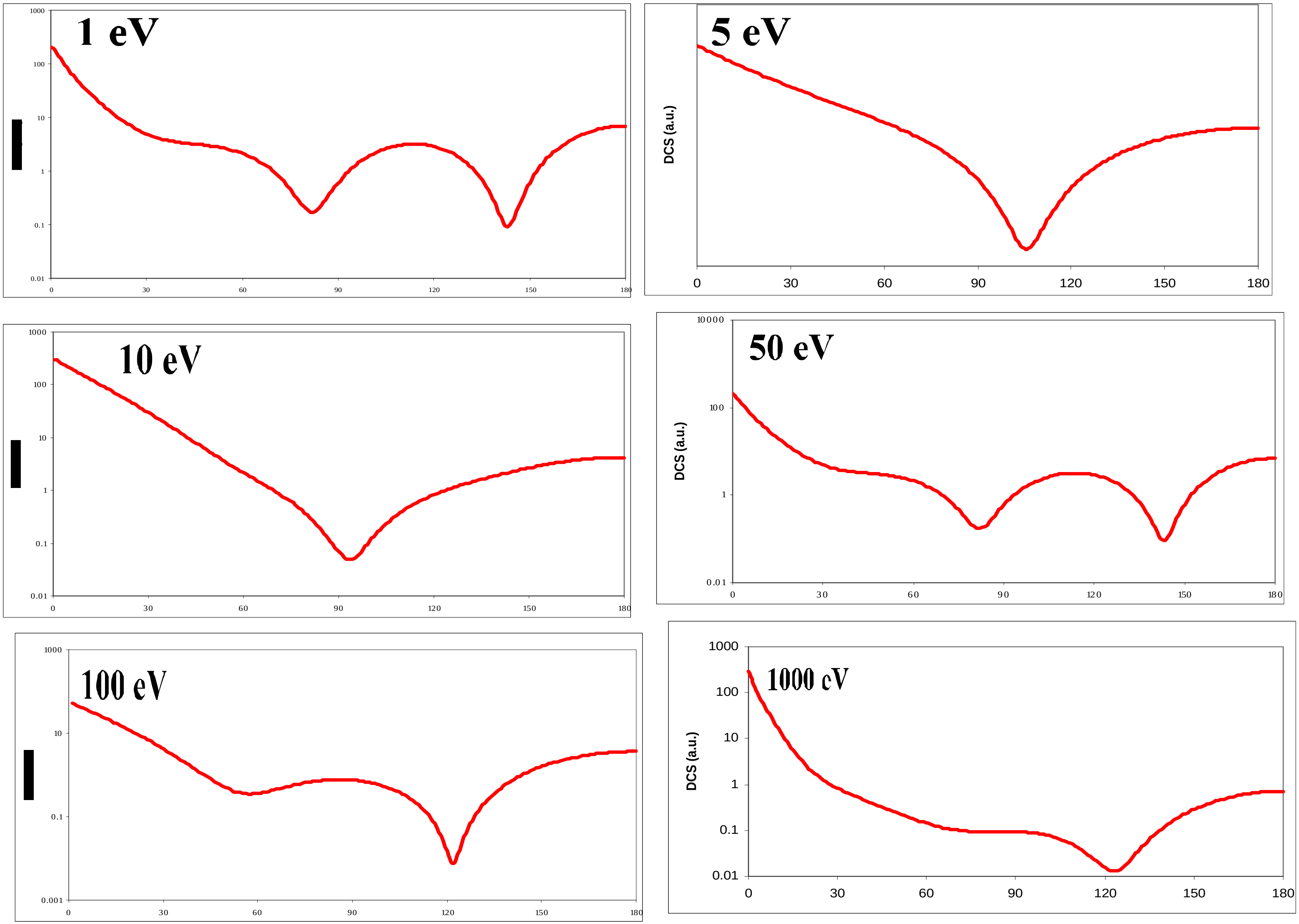

1 eV
1000
100
10
1
0.1
0.01
0
30
60
90
120
150
180
[redacted]
5 eV
DCS (a.u.)
0
30
60
90
120
150
180
10 eV
1000
100
10
1
0.1
0.01
0
30
60
90
120
150
180
[redacted]
50 eV
DCS (a.u.)
10000
100
1
0.01
0
30
60
90
120
150
180
100 eV
1000
10
0.1
0.001
0
30
60
90
120
150
180
[redacted]
1000 eV
DCS (a.u.)
1000
100
10
1
0.1
0.01
0
30
60
90
120
150
180

Hg

Mercury

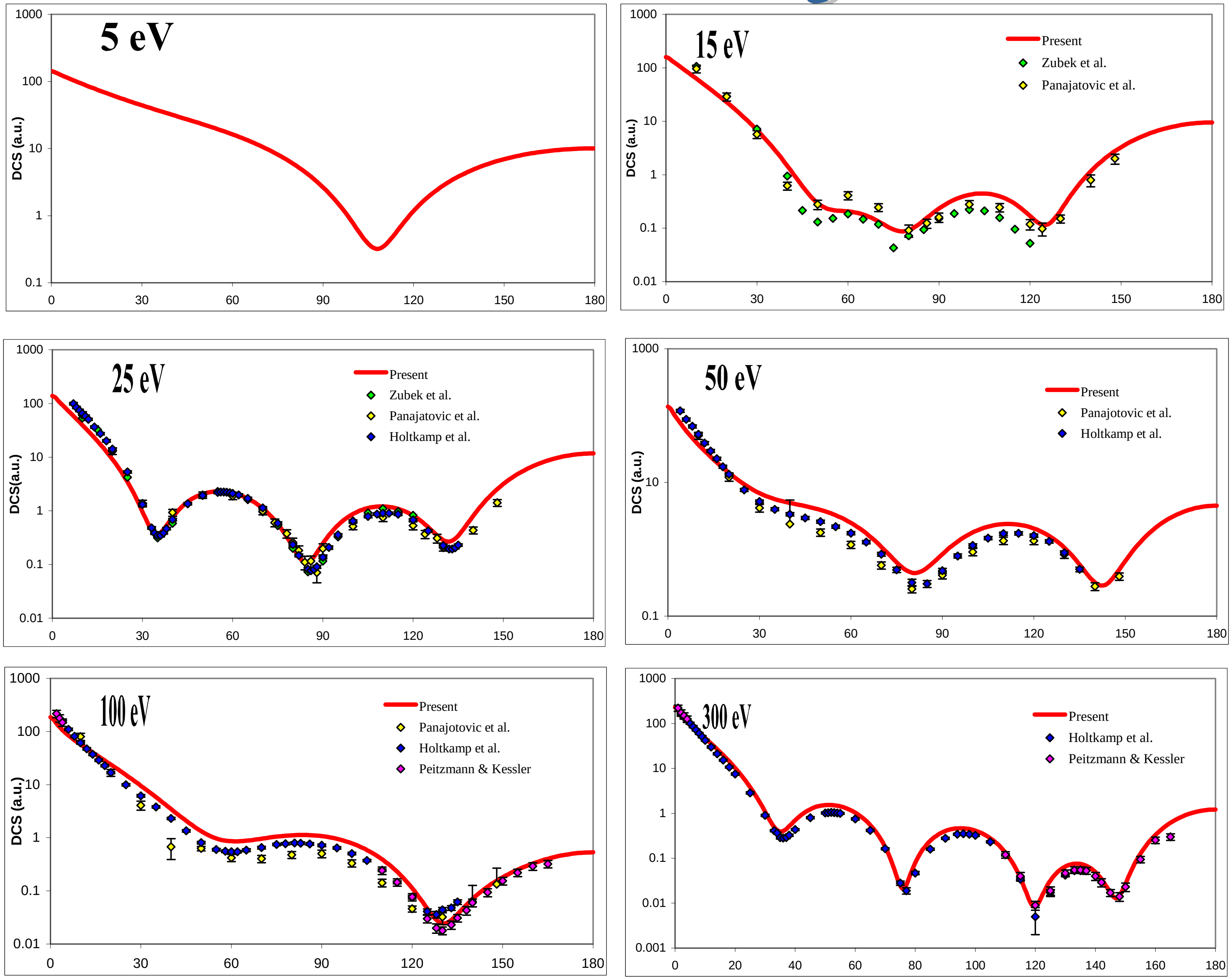

5 eV
DCS (a.u.)
1000
100
10
1
0.1
0
30
60
90
120
150
180
15 eV
Present
Zubek et al.
Panajatovic et al.
DCS (a.u.)
1000
100
10
1
0.1
0.01
0
30
60
90
120
150
180
25 eV
Present
Zubek et al.
Panajatovic et al.
Holtkamp et al.
DCS(a.u.)
1000
100
10
1
0.1
0.01
0
30
60
90
120
150
180
50 eV
Present
Panajotovic et al.
Holtkamp et al.
DCS (a.u.)
1000
10
0.1
0
30
60
90
120
150
180
100 eV
Present
Panajotovic et al.
Holtkamp et al.
Peitzmann & Kessler
DCS (a.u.)
1000
100
10
1
0.1
0.01
0
30
60
90
120
150
180
300 eV
Present
Holtkamp et al.
Peitzmann & Kessler
1000
100
10
1
0.1
0.01
0.001
0
20
40
60
80
100
120
140
160
180